Low-Chattering Discretization of Sliding Modes

Avi Hanan, Adam Jbara and Arie Levant
in ”Sliding-Mode Control and Variable-Structure Systems: The State of the Art”
Springer International Publishing, 2023, pp. 229-264

Abstract Sliding mode control (SMC) is known for its efficacy and robustness, but also features the notorious chattering effect both in applications and simulation. The new control-discretization method diminishes the chattering while preserving the system trajectories, accuracy and insensitivity to matched disturbances. The unavoidable restrictions of low-chattering SMC discretization methods are discussed. Computer simulation demonstrates visual chattering removal.

1 Introduction

Sliding-mode (SM) control (SMC) [56, 59, 60] is widely used in control of uncertain systems. For this end a proper constraint $\sigma = 0$ is chosen to be exactly kept, where σ is some (often virtual) output available in real time. The constraint $\sigma = 0$ is kept by high-frequency control switching preventing any deviation of σ from 0, and the closed system is said to be in SM. As a result, SMC suppresses system uncertainties corresponding to bounded disturbances in the control channel, which results in the high overall system performance. The relative degree of the output σ defines the SM order [32, 33, 56].

Avi Hanan (e-mail: `avih@tauex.tau.ac.il`), Adam Jbara (e-mail: `adamjbara@tauex.tau.ac.il`), Arie Levant (e-mail: `levant@tauex.tau.ac.il`) are with
Tel-Aviv University, Tel Aviv, 6997801 Tel-Aviv, Israel

Unfortunately, SMC also can induce dangerous system vibrations (the chattering effect) due to the switching combined with discrete noisy sampling and/or parasitic dynamics [6, 8, 36]. Three main methods broadly used for alleviating these vibrations are SM regularization, dynamic extension (artificially increasing the relative-degree [27]), and SMC discretization specially adjusted to lower vibrations.

SM regularization replaces relays with some continuous ("sigmoid") approximations [59]. It actually introduces a local singular perturbation. As the result the high SM accuracy and the dynamics insensitivity to matched disturbances are partially destroyed. Moreover, the chattering due to the discrete noisy sampling is amplified.

The second method, dynamic extension, adds integrators into the feedback, and requires application of high-order SM (HOSM) control (HOSMC) [32, 57, 58]. Such HOSMC indeed establishes and keeps constraints of any relative degrees and is capable of significantly diminishing the chattering [4, 33, 36]. In fact, in that case the discontinuous control derivative suppresses the derivatives of the uncertain matched disturbance. Correspondingly, only smooth matched disturbances are removable, and higher-order derivatives of σ turn into new system states to be estimated in real time. Also the recently proposed integral-action method [45] suffers of a similar information deficiency.

This paper studies low-chattering discretization methods remaining "faithfull" to the original discontinuous system dynamics.

In the sequel by ***discretization*** *we mean replacing the original continuous-time dynamic system or some of its subsystems with discrete-time counterparts. The ultimate requirement is that the solutions and the trajectories of the resulting hybrid system converge to the solutions and the trajectories of the original system, as the maximal discretization time interval vanishes.*

That formulation is intentionally vague in order to cover most of currently available discretization methods. This paper studies finite-dimensional systems and the corresponding discretized solutions uniformly converge to the theoretically established ideal continuous-time solutions over each closed time interval. The explicit dependence of the obtained solutions on the sampling/discretization time step separates the discretization from the first two methods.

Note that, generally speaking, the chattering due to sampling noises [36] is only reducible at the cost of significant performance degradation. Indeed, one cannot distinguish output varying due to sampling noises from the actual state variations. Also high-frequency internal system vibrations all but assure its chattering independently of applied chattering-reduction methods.

Traditional discretizations of discontinuous systems employ the (explicit) Euler method, and usually result in significant chattering [16]. Implicit discretization methods [1, 9, 10, 12, 26, 49] develop special Euler-method modifications to resolve the issue.

The traditional Euler discretization can be described as the one-step forwards-in-time recursion, which is repeated at each sampling/discretization time step. That discretization is used either for the numeric simulation of a closed-loop system, or for determining the next control injection value in real-time applications. In the latter case the input makes use of discretely sampled noisy outputs. Much more advanced methods, like Runge-Kutta methods, are not available if the dynamics are discontinuous or even only non-smooth.

The implicit Euler procedure corresponds to the above Euler recursion repeatedly applied *backwards in time* at each successive step in the normal forwards-in-time direction. In practice it means solving the Euler recursion equation for the unknown future system state at each integration/sampling time instant. The method theoretically requires the knowledge of the exact mathematical system model and numerically solving nontrivial equations at each discretization time step. The algorithm indeed suppresses the chattering of smooth switched systems in the absence of sampling noises, since the moment when the trajectory enters the SM is predicted in advance, and, starting from that moment, the SM motion is driven by the standard smooth Filippov SM dynamics.

Unfortunately, in reality such exact model knowledge is mostly not possible. The obstacle is overcome by some short-time approximate state prediction, and using set-valued functions instead of discontinuities. The approach invokes some beautiful mathematics [11, 26, 29, 30, 31, 47, 48, 61]. Such *semi-implicit* methods still inevitably assume a sufficiently detailed system model and the sampling step known in advance. They are especially effective for the first-order SMs, but higher-order SM applications are also known [9, 10, 50]. The realization for higher relative degrees might become complicated due to repeated numeric solutions of nonlinear algebraic equations. These numeric procedures often also prevent accurately estimating the system accuracy due to sampling noises.

This paper further develops a novel simple discretization approach [23] to the Filippov dynamics [18]. The method preserves the continuous-time system trajectories and accuracy asymptotics, it also does not cause performance degradation. Similarly to the above methods it still depends on the control structure, but that dependence is much weaker.

Only standard SMC uncertainty conditions are imposed for any relative degrees and SM orders, the sampling periods can be unknown and variable. The real-time discretization recursion step is always described by analytic formulas developed in advance. The procedure does not involve on-line numerical solutions of equations.

Utilizing this approach, we have recently proposed simple low-chattering discretizations of SM-based filtering differentiators [25], and have found proper parametric sets for these differentiators up to the order 12.

In the following we develop low-chattering discretizations for two families of *arbitrary-order* homogeneous SM controllers [14], as well as of the twisting controller [32]. Furthermore, the method has been recently extended [24] to the complicated case of ”recursive” (nested) SMs [33] (not covered by this chapter). In all cases only the standard SMC uncertainty conditions are imposed. In the output-feedback format the new scheme utilizes the above low-chattering discrete differentiators [25]. The simplicity and the efficacy of the method is validated by extensive computer experiments.

Notation[1]. Let $\mathrm{sat}\, s = \max[-1, \min(1, s)]$. We use the widely-accepted special power function $\lfloor \cdot \rceil^m = |\cdot|^m \,\mathrm{sign}(\cdot)$, $m \geq 0$. The norm $||x||$ stays for the standard Euclidean norm of x, $B_\varepsilon = \{x|\; ||x|| \leq \varepsilon\}$, correspondingly $||x||_h$ is a homogeneous norm, $B_{h\varepsilon} = \{x|\; ||x||_h \leq \varepsilon\}$.

A function of a set is the set of function values on this set. Let $a \diamond b$ be a binary operation for $a \in A, b \in B$, then $A \diamond B = \{a \diamond b | a \in A, b \in B\}$.

Depending on the context, we use the same notation $\vec{\xi}_k$ for both $(\xi, \dot{\xi}, ..., \xi^{(k)})$ and $(\xi_0, \xi_1, ..., \xi_k)$. The finite-difference operator $\delta_j A = A(t_{j+1}) - A(t_j)$ is introduced for any sampled function $A(t_j)$.

2 Discontinuous dynamic systems

Recall a few notions[2].

Let $T\mathbb{R}^{n_x}$ stay for the tangent space to $\mathbb{R}^{n_x}$, and $T_x\mathbb{R}^{n_x}$ denote the tangent space at the point $x \in \mathbb{R}^{n_x}$. Consider the differential inclusion (DI)

$$\dot{x} \in F(x),\; x \in \mathbb{R}^{n_x}, F(x) \subset T_x\mathbb{R}^{n_x}. \tag{1}$$

As usual, solutions of (1) are defined as locally absolutely-continuous functions $x(t)$, satisfying DI (1) for almost all t.

Note that whereas the right-hand side of (1) is often assumed embedded in $\mathbb{R}^{n_x}$ [27, 18, 52], we need the tangent-space formalism for the homogeneity considerations (see the Appendix).

We call a differential inclusion (DI) (1) *Filippov DI*, if the right-hand vector set $F(x)$ is non-empty, compact and convex for any x, and F is an upper-semicontinuous set-valued function of x [18, 34]. The upper-semicontinuity of F means that the maximal distance of the vectors of $F(x)$ from the vector set $F(y)$ tends to zero as x approaches y.

Solutions of the Filippov DIs feature most of the usual properties including the existence of a local solution for the Couchy problem, and solutions' extendability till the boundary of a compact region. Naturally, solutions are not unique, but the solutions still continuously depend on the right-hand side of (1). More important is that, in fact, they continuously depend on the *graph* of the DI [18].

Consider a differential equation (DE) $\dot{x} = f(x), x \in \mathbb{R}^{n_x}$, with a locally essentially bounded Lebesgue-measurable right-hand side $f : \mathbb{R}^{n_x} \to T\mathbb{R}^{n_x}$. It is understood *in the Filippov sense* [18], if its solutions are defined as the solutions of the special DI $\dot{x} \in K_F[f](x)$ for

[1] Notation is reprinted from the papers [21, 23] by authors with the permission by Springer Nature and IEEE.

[2] Notions and notation introduced here are standard and reprinted from the papers [21, 23] by authors with the permission by Springer Nature and IEEE.

$$K_F[f](x) = \bigcap_{\mu_L N=0} \bigcap_{\delta>0} \overline{co}\, f((x+B_\delta)\backslash N). \tag{2}$$

Here $\overline{\text{co}}$ denotes the convex closure, whereas μ_L stays for the Lebesgue measure.

Formula (2) introduces the famous Filippov procedure, and the corresponding DI $\dot{x} \in K_F[f](x)$ is a Filippov DI [18]. In the sequel in the non-autonomous case we add the virtual coordinate t, $\dot{t} = 1$.

Filippov solutions satisfy all widely accepted alternative definitions for solutions of discontinuous dynamic systems. Actually they constitute the minimal set of such solutions.

The graph $\Gamma(F)$ of the DI (1) over the domain $G \subset \mathbb{R}^{n_x}$ is defined as the set of pairs $\Gamma(F) = \{(x,\xi) \mid x \in G,\ \xi \in F(x)\}$. In spite of $\Gamma(F) \subset \mathbb{R}^{n_x} \times T\mathbb{R}^{n_x}$, it is locally topologically isomorphically embedded in $\mathbb{R}^{2n_x}$ for any fixed coordinates.

Let G be closed, and $F(x)$ be nonempty, compact and locally bounded for any $x \in G$, then F is upper-semicontinuous in G if and only if $\Gamma(F)$ is closed [18]. Furthermore, if F is upper-semicontinuous and G is compact, then also $\Gamma(F)$ is compact [18]. In other words, Filippov's procedure generates the minimal convex closure of the original DE graph (Fig. 1).

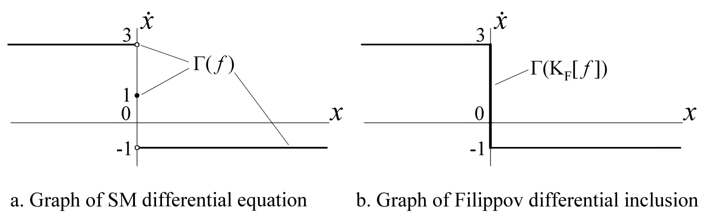

Fig. 1 Filippov procedure. a: Graph $\Gamma(f)$ of the DE $\dot{x} = f(x) = 1 - 2\,\mathrm{sign}\,x$. b: Graph of the corresponding Filippov inclusion.

The set of solutions for the Filippov DI (1) defined over the segment $[a,b]$, $a \le 0 \le b$, for initial conditions $x(0)$ within a fixed compact set $\Omega \subset \mathbb{R}^{n_x}$, $x(0) \in \Omega$, is compact in the C-metric. Moreover, the points of the corresponding trajectories constitute a compact set in $\mathbb{R}^{n_x}$.

In the usual case when a function ϕ is continuous almost everywhere, the set $K_F[\phi](x)$ is the convex closure of the limit values $\lim_{k\to\infty} \phi(y_k)$ obtained along all possible continuity-point sequences y_k approaching x.

Approximation of solutions. A locally absolutely-continuous function $\xi : I \to G$ is further called a δ-graph-approximating (δ-GA) solution of the Filippov DI (1) over the closed domain $G \subset \mathbb{R}^{n_x}$, $\delta \ge 0$, $I \subset \mathbb{R}$, if it satisfies $(\xi(t), \dot{\xi}(t)) \in \Gamma(F) + B_\delta$ for almost all $t \in I$. The time interval I here can be open, one-side-open or closed, finite or infinite.

In the case of the compact time interval I and any $\varepsilon > 0$ there exists $\delta > 0$ such that every δ-GA solution of the Filippov DI (1) defined over I in a closed region $G \subset \mathbb{R}^{n_x}$ is C-metric distanced by not more than ε from a solution of DI (1). Vice versa, if $\delta_k \to 0$, then any sequence of δ_k-GA solutions has a subsequence which uniformly converges to a solution of (1) over I [18].

Stability Notions. A point $x_0 \in \mathbb{R}^{n_x}$ is termed the equilibrium of the Filippov DI (1), if the constant function $x(t) \equiv x_0$ satisfies it. The equilibrium x_0 is (Lyapunov) stable, if each solution starting in some its vicinity $||x(0) - x_0|| < \delta_0$ at $t = 0$ is extendable till infinity in time, and for any $\varepsilon > 0$ there exists such $\delta > 0$, $\delta \leq \delta_0$, that any solution $x(t)$ satisfying $||x(0) - x_0|| < \delta$ satisfies $||x(t) - x_0|| < \varepsilon$ for any $t \geq 0$.

A stable equilibrium x_0 is called asymptotically stable (AS), if any solution $x(t)$ starting in some its vicinity satisfies $\lim_{t\to\infty} ||x(t) - x_0|| = 0$. It is globally AS if $\lim_{t\to\infty} ||x(t) - x_0|| = 0$ for any $x(0) \in \mathbb{R}^{n_x}$.

An AS equilibrium x_0 is called *finite-time (FT) stable* (FTS), if x_0 is AS, and for each initial condition $x(0)$ from some vicinity of x_0 there exists such a number $T \geq 0$ that $x(t) \equiv x_0$ for any $t \geq T$. It is called *globally FTS*, if such T exists for any initial condition $x(0) \in \mathbb{R}^{n_x}$. The equilibrium x_0 is termed *fixed-time (FxT) stable* (FxTS) [51, 55, 54], if it is globally FTS and there is an upper transient-time *constant* bound $T > 0$ valid for all solutions and initial conditions.

Locally (globally) AS autonomous Filippov DIs possess proper local (global) smooth Lyapunov functions [13].

3 Discretization of Filippov dynamic systems

In this section we introduce a new simple discretization method. Let the controlled system $\dot{x} = X(t, x, u)$ have the output $\sigma \in \mathbb{R}^{n_s}$. Consider a general closed-loop system

$$\begin{array}{l} \dot{x} = X(t, x, u_1, u_2),\ x \in \mathbb{R}^{n_x},\ u_1 \in \mathbb{R}^{n_{u1}},\ u_2 \in \mathbb{R}^{n_{u2}}, \\ \dot{u}_1 = U_1(t, x, u_1, u_2, \sigma(t, x)),\ u_2 = U_2(t, u_1, \sigma(t, x)), \end{array} \tag{3}$$

with a general-form output feedback, locally bounded and Lebesgue-measurable X locally bounded and Borel-measurable functions U_1, U_2.

Let the system be understood in the Filippov sense, and the corresponding Filippov DI be

$$\tfrac{d}{dt}(t, x, u_1)^T \in F_{txu}(t, x, u_1). \tag{4}$$

Let $\bar{t}_d = \{t_j\} = t_0, t_1, ...$ be the sequence of sampling time instants, $t_j < t_{j+1}$, $\tau_j = t_{j+1} - t_j$, where $t_j \in [t_a, t_b]$. Let $\sup_j \tau_j \leq \tau$, where τ is called the *discretization density* of $\bar{t}_d$. Assume that such sampling-time sequences exist for any density $\tau > 0$.

A discretization of the closed-loop system (3) is further defined as any algorithm producing $\delta(\bar{t}_d)$-GA solutions of the corresponding Filippov DI (4) which converge to its solutions as the sampling density τ vanishes.

There are two natural types of discretization: the discretization of the whole system corresponding to the computer simulation, and the feedback discretization leaving the continuous-time system dynamics intact. The latter models practical applications and results in a hybrid system of the form

$$\begin{aligned}&\dot{x} = X(t, x, u_1, u_2),\ x \in \mathbb{R}^{n_x},\ u_1 \in \mathbb{R}^{n_{u1}},\ u_2 \in \mathbb{R}^{n_{u2}},\\&\dot{u}_1 = U_{1d}(t, x, u_1(t_j), \sigma(t_j, x(t_j)), \tau, \tau_j),\ t \in [t_j, t_{j+1}),\ j = 0, 1, ...,\\&u_2 = U_{2d}(t_j, u_1(t_j), \sigma(t_j, x(t_j)), \tau, \tau_j),\end{aligned} \tag{5}$$

where U_{1d}, U_{2d} are some discretized controls replacing U_1, U_2. The following theorem is a direct corollary of the above Filippov results (Fig. 2a).

Theorem 1. *Let the right-hand side of* (5) *be distanced by not more than* $\delta_\tau \geq 0$ *from the graph* $\Gamma(F_{txu})$ *of the Filippov DI* (4) *over a compact set* $\Omega \subset \mathbb{R}^{n_x+n_{u1}+1}$*, and* δ_τ *depend on the discretization density* τ *and tend to* 0 *as* $\tau \to 0$*. Consider the set of solutions for* (5) *(discretized solutions) taking initial values in a compact subset* Ω_0*,* $(t_0, x(t_0), u_1(t_0)) \in \Omega_0 \subset \Omega$*, defined over a fixed time segment* $[t_a, t_b]$*,* $t_0 \in [t_a, t_b]$*, and staying in the region,* $(t, x(t), y(t)) \in \Omega$*, for* $t \in [t_a, t_b]$*. Then these solutions uniformly converge to the set of solutions of* (4) *as* $\tau \to 0$*.*

A theorem similar to Theorem 1 holds provided the discretization is extended to the closed-loop dynamics of the whole state (computer simulation case).

Remark. *It follows from Theorem 1 that one can try any reasonable discretization of a system without risking its destruction or performance degradation. It is a great feature for practical implementation.*

On the other hand, the chattering attenuation proof is often complicated, since the very chattering notion is vague, and the criteria are only qualitative [36].

Neither the vibration magnitude, nor its frequency, or both of them do determine the chattering intensity. That is why all chattering reduction methods usually only contain the proof of the system stability, and, sometimes, the convergence of the solutions to the ideal ones. No general formal claims of the chattering removal can be formulated. In particular, basic proven results for the implicit Euler discretization are reducible to the system asymptotic-stability preservation and robustness with respect to certain disturbances. The accuracy in the presence of noises is usually experimentally estimated.

In the following we demonstrate that a proper simple feedback discretization can significantly diminish the system chattering in the absence of noises, or when the noises are small (usually very small). Note once more that in general it is not possible to remove the chattering caused by sampling noises.

3.1 Example: alternative discretization of relay control

Note that a general discretization of the first-order SMC is considered as a simple particular case in Section 5. Consider the scalar SMC scalar system

$$\dot{x} = h(t) + g(t)u,\ u = -2\,\mathrm{sign}\,x; \tag{6}$$

The graph of the closed-loop system (6) for $h = g = 1, f = h + gu$ is shown in Fig. 1a, while the graph of the corresponding Filippov DI appears in 1b. It contains the vertical segment $[-1, 3]$ at $x = 0$.

According to Theorem 1 we are to choose a proper value (selector) of $\dot{x}(t_j)$ for each Euler step

$$\begin{array}{l} x(t_{j+1}) = x(t_j) + \dot{x}(t_j)\tau_j,\ 0 < \tau_j \leq \tau, \\ (x(t_j), \dot{x}(t_j)) \in \Gamma(K_F(f)) + B_{\varepsilon(\tau)},\ \lim_{\tau\to 0} \varepsilon(\tau) = 0, \end{array} \tag{7}$$

providing for reasonably smooth convergence of $(x(t_j), \dot{x}(t_j))$ to an infinitesimally small vicinity of $0 \in \mathbb{R}^2$ or even asymptotic convergence to 0 for each sampling density τ (Fig. 2a).

Let now $\tau > 0$ be small, and choose some $k_0 \geq 0$. Replace the vertical segment with a thin vertical rectangle of the width $2k_0\tau$ obtaining the new Filippov DI

$$\begin{array}{l} h(t) = 1,\ g(t) = 1, \\ \dot{x} \in \begin{cases} \{-1\} \text{ for } x > k_0\tau, \\ [-1, 3] \text{ for } |x| \leq k_0\tau, \\ \{3\} \text{ for } x < -k_0\tau. \end{cases} \end{array} \tag{8}$$

The graph of the DI (8) obviously lies inside the "swelled" graph $\Gamma(K_F(f)) + B_\varepsilon$ for $\varepsilon = k_0\tau$ (Fig. 2a).

Assign the values $\dot{x}(t_j)$ from the inclusion (8). According to Theorem 1 differently choosing $k_0 \geq 0$ and $\dot{x}(t_j)$ obtain different discretization schemes.

The standard Euler discretization of (6) corresponds to $k_0 = 0$ (Fig. 2b),

$$x(t_{j+1}) = x(t_j) + (1 - 2\,\mathrm{sign}\,x(t_j))\tau_j. \tag{9}$$

The simple alternative discretization

$$x(t_{j+1}) = x(t_j) + \mathrm{sat}\left(\frac{|x(t_j)|}{|2\,\mathrm{sign}\,x(t_j) - 1|\tau_j}\right)(1 - 2\,\mathrm{sign}\,x(t_j))\tau_j \tag{10}$$

steers $x(t)$ to 0 in finite time (FT) and corresponds to $k_0 \geq 3$ (Fig. 2c). It requires the exact knowledge of the system.

Another alternative discretization,

$$x(t_{j+1}) = x(t_j) + [h(t_j) + g(t_j)u(t_j)]\tau_j,\ u(t_j) = -2\,\mathrm{sat}\left(\frac{x(t_j)}{4\tau}\right), \tag{11}$$

corresponds to $k_0 \geq 4$ and asymptotically stabilizes the system (6) for $h = g = 1$ (Fig. 2d).

Moreover, scheme (11) remains effective for any $h(t) \in [-1, 1]$, $g(t) \in [1, 1.5]$, in which case $x(t)$ converges into a vicinity of zero. The equality $x(t) = -\frac{\tau}{4}\frac{h(t)}{g(t)} + O(\tau^2)$ is kept, provided the equivalent control $u_{eq} = -h/g$ and its derivatives $\dot{u}_{eq}, \ddot{u}_{eq}$ are bounded, $|u_{eq}| \leq \text{const} < 2$. Any $k_0 > 3$ corresponds to the scheme.

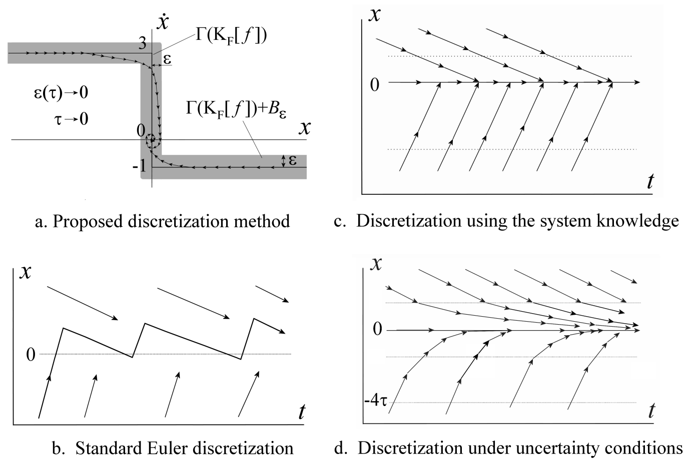

Fig. 2 First-order SMC (6) for $h = g = 1$ and its discretizations. a: The proposed discretization method for $\dot{x} = f(x) = 1 - 2\,\mathrm{sign}\,x$. b: The standard Euler discretization (9). c: Alternative discretization (10) utilizing the knowledge of the system provides for the FT stability. d: Alternative discretization (11) is effective for any h, g, $|h| \leq 1$, $|g| \in [1, 1.5]$ and provides for the asymptotic stability for $h = g = 1$.

The discretized control of (11) also stays effective for the continuous-time system (6) (see Section 5). Obviously one can propose many other low-chattering discretization schemes for the relay control.

4 Homogeneous output regulation

The natural way of implementing the proposed discretization method is local in time and state (Theorem 1). A system homogeneity (see the Appendix) extends the system features from any vicinity of the origin to the whole state space. Correspondingly the homogeneity allows extending any system treatment including discretization to the whole space [50]. Unfortunately effective discretization still depends on the structure of the concrete systems and/or controllers.

In the following we introduce the standard SMC problem and the concrete homogeneous single-input single-output (SISO) SM controllers [14] to be discretized in the sequel.

Standard SMC problem [33]. Let the dynamic system be

$$\dot{x} = a(t,x) + b(t,x)u, \;\; \sigma = \sigma(t,x), \tag{12}$$

where $x \in \mathbb{R}^n$, $a : \mathbb{R}^{n+1} \to T_x\mathbb{R}^n$, $b : \mathbb{R}^{n+1} \to T_x\mathbb{R}^n$ and $\sigma : \mathbb{R}^{n+1} \to \mathbb{R}$ are uncertain smooth functions, $u \in \mathbb{R}$ is the control. The output σ might, for example, be a tracking error.

Solutions of (12) are understood in the Filippov sense, which allows application of discontinuous controls $u(t,x)$. For simplicity any solution of (12) is assumed forward complete (i.e. extendable in time till infinity), provided the corresponding control function of time $u(t,x(t))$ stays bounded along the solution $x(t)$.

System (12) is assumed to have a constant relative degree r [27]. It means that

$$\sigma^{(r)} = h(t,x) + g(t,x)u, \tag{13}$$

holds, where the function g does never vanish [27]. Traditionally for SMC smooth functions $h(t,x)$ and $g(t,x)$ are assumed unknown, but bounded and satisfying the conditions

$$|h(t,x)| \leq C,\; 0 < K_m \leq g(t,x) \leq K_M. \tag{14}$$

where $C, K_m, K_M > 0$, as well as $r \geq 1$, are the problem parameters.

The SMC task is to establish and keep the constraint $\sigma \equiv 0$.

Obviously, the uncertain dynamics (13), (14) imply the quite certain DI

$$\sigma^{(r)} \in [-C, C] + [K_m, K_M]u. \tag{15}$$

Denote $\vec{\sigma}_k = (\sigma, \dot{\sigma}, \ldots, \sigma^{(k)}) \in \mathbb{R}^{k+1}$. Introduce some discontinuous SMC

$$u = \alpha u_{*r}(\vec{\sigma}_{r-1}). \tag{16}$$

The mode $\sigma(t,x(t)) \equiv 0$ is further called rth-order SM (r-SM) [32, 33] if the corresponding r-SM set $\vec{\sigma}_{r-1} = 0$ locally or globally is the integral set of the Filippov DE (12). Provided the r-SM set is an attracting forward-invariant set, controller (16) is called r-SM controller (r-SMC further stays for both "r-SM controller" or "r-SM control") .

In particular, due to their form, the following control is called the "rational" r-SMC [14],

$$u_{*r} = u_{Qr}(\vec{\sigma}_{r-1}) = -\frac{\lfloor\sigma^{(r-1)}\rceil^{\frac{1}{1}} + \beta_{r-2}\lfloor\sigma^{(r-2)}\rceil^{\frac{1}{2}} + \ldots + \beta_0\lfloor\sigma\rceil^{\frac{1}{r}}}{|\sigma^{(r-1)}|^{\frac{1}{1}} + \beta_{r-2}|\sigma^{(r-2)}|^{\frac{1}{2}} + \ldots + \beta_0|\sigma|^{\frac{1}{r}}}, \tag{17}$$

whereas the next one is the "relay" r-SMC [14],

$$u_{*r} = u_{Sr}(\vec{\sigma}_{r-1}) = -\operatorname{sign}\left[\left\lfloor\sigma^{(r-1)}\right\rceil^{\frac{1}{1}} + \beta_{r-2}\left\lfloor\sigma^{(r-2)}\right\rceil^{\frac{1}{2}} + \ldots + \beta_0\lfloor\sigma\rceil^{\frac{1}{r}}\right]. \tag{18}$$

Both controllers (17), (18) establish and keep the r-SM $\sigma = 0$ for the same properly chosen parametric set $\beta_0, \ldots, \beta_{r-2} > 0$, whereas the parameter $\alpha > 0$ is taken large enough, but different for u_{Qr} and u_{Sr}. Naturally, $\alpha > 0$ equals the magnitude of the control.

The value of $u_{Qr}(0)$ is defined voluntarily, for it does not affect the Filippov solutions (2). Note that in the both cases get $u_{*1} = -\operatorname{sign}\sigma$ for $r = 1$.

Obviously the rational control (17) is continuous everywhere except $\vec{\sigma}_{r-1} = 0$. Such controls are called *quasi-continuous* (QC) [35] (see the Appendix). Contrary to that the discontinuity set $u_{Qr} = 0$ of the relay controller is comprised of subsurfaces occasionally possessing infinite gradients. Hence, during the transient control (18) cannot keep $u_{Qr} = 0$ in SM at such points, nevertheless, temporary SMs $u_{Qr} = 0$ can arise over some time intervals.

Correspondingly, solutions of (12), (16), (14) satisfy the resulting Filippov DI

$$\sigma^{(r)} \in [-C, C] + \alpha[K_m, K_M] K_F[u_{*r}](\vec{\sigma}_{r-1}). \tag{19}$$

Obviously these controls require the availability or the real-time estimation of $r-1$ derivatives $\dot{\sigma}, ..., \sigma^{(r-1)}$.

Further any continuous-time (possibly discontinuous) feedback control in DIs is assumed replaced by the result of its Filippov procedure (2).

Assigning the weights $\deg \sigma^{(i)} = r - i$ renders DI (19) homogeneous of the homogeneity degree (HD) -1, $-\deg t = -1$ (see the Appendix [34]). Obviously $\deg \sigma^{(r)} = \deg u_{*r} = 0$. Assume that the sampling-noise magnitude and the sampling time period do never exceed $\varepsilon_0 \geq 0$ and $\tau > 0$ respectively. Then the homogeneity implies that the accuracy [34]

$$|\sigma^{(i)}| \leq \mu_i \rho^{r-i} \tag{20}$$

is established in FT and kept for some constants $\mu_i > 0$ and $\rho = \max[\tau, \varepsilon_0^{1/r}]$. Formula (20) is also correct for sampling in continuous time, $\tau = 0$, for possibly-different coefficients μ_i.

4.1 Differentiation and filtering based on SMs

SMC technique traditionally requires differentiation of the sliding variable[3].

Let $\mathrm{Lip}_{n_d} L$ stay for the set of all scalar functions $\phi : \mathbb{R}_+ \to \mathbb{R}$, $\mathbb{R}_+ = [0, \infty)$, possessing Lipschitzian n_dth derivative with the Lipschitz constant $L > 0$. It implies that $|\phi^{(n_d+1)}| \leq L$ holds for almost all $t \in \mathbb{R}_+$.

Let the sampled input signal $f(t)$, $t \geq 0$, be of the form $f(t) = f_0(t) + \eta(t)$, where $f_0 \in \mathrm{Lip}_{n_d} L$ is the unknown basic signal to be differentiated and $\eta(t)$ is a Lebesgue-measurable noise.

The numbers L, n_d are assumed known, and the function $f(t)$ is available (sampled) in real time.

An n_dth-order differentiator, $n_d \geq 0$, is defined as any algorithm producing functions $z_0, ..., z_{n_d} : \mathbb{R}_+ \to \mathbb{R}$. Functions $z_i(t)$, $i = 0, 1, ..., n_d$, are assumed to have the sense of the real-time estimations for $f_0^{(i)}(t)$.

[3] Some notions and notation introduced here are reprinted from the papers [21, 23] by authors with the permission by Springer Nature and IEEE.

Let a differentiator be exact after some FT transient on all inputs $f = f_0 \in \mathrm{Lip}_{n_d} L$ for $\eta(t) \equiv 0$. Then it is called **asymptotically optimal** [42], if for some $\mu_i > 0$, any $f_0 \in \mathrm{Lip}_{n_d}(L)$, any $\varepsilon_0 \geq 0$, and any bounded Lebesque-measurable noise η, $\operatorname{ess\,sup} |\eta(t)| \leq \varepsilon_0$, it in FT establishes the differentiation accuracy

$$|z_i(t) - f_0^{(i)}(t)| \leq \mu_i L^{\frac{i}{n_d+1}} \varepsilon_0^{\frac{n_d+1-i}{n_d+1}}, \; i = 0, 1, ..., n_d. \tag{21}$$

Accuracy asymptotics (21) are proved to be the best possible for bounded noises [42]. It is also proved there that $\mu_i \geq 2^{\frac{i}{n_d+1}}$ always holds, $i = 0, ..., n_d$. Arbitrary-order asymptotically-optimal differentiators were for the first time proposed in [33], and they are SM-based.

The filtering differentiator [43, 41] of the differentiation order $n_d \geq 0$ and the filtering order $n_f \geq 0$ has the form

$$\begin{aligned}
\dot{w}_1 &= -\tilde{\lambda}_{n_d+n_f} L^{\frac{1}{n_d+n_f+1}} \lfloor w_1 \rceil^{\frac{n_d+n_f}{n_d+n_f+1}} + w_2, \\
&\dots \\
\dot{w}_{n_f-1} &= -\tilde{\lambda}_{n_d+2} L^{\frac{n_f-1}{n_d+n_f+1}} \lfloor w_1 \rceil^{\frac{n_d+2}{n_d+n_f+1}} + w_{n_f}, \\
\dot{w}_{n_f} &= -\tilde{\lambda}_{n_d+1} L^{\frac{n_f}{n_d+n_f+1}} \lfloor w_1 \rceil^{\frac{n_d+1}{n_d+n_f+1}} + w_{n_f+1}, \\
w_{n_f+1} &= z_0 - f(t),
\end{aligned} \tag{22}$$

$$\begin{aligned}
\dot{z}_0 &= -\tilde{\lambda}_{n_d} L^{\frac{n_f+1}{n_d+n_f+1}} \lfloor w_1 \rceil^{\frac{n_d}{n_d+n_f+1}} + z_1, \\
&\dots \\
\dot{z}_{n_d-1} &= -\tilde{\lambda}_1 L^{\frac{n_d+n_f}{n_d+n_f+1}} \lfloor w_1 \rceil^{\frac{1}{n_d+n_f+1}} + z_{n_d}, \\
\dot{z}_{n_d} &= -\tilde{\lambda}_0 L \,\mathrm{sign}(w_1), \; |f_0^{(n_d+1)}| \leq L.
\end{aligned} \tag{23}$$

It also features strong noise-filtering capabilities [41, 25]. In particular, it filters out even *unbounded* noises, provided their local iterated integrals of an order not exceeding n_f are small [41]. Moreover, differentiator (27) directly extracts the equivalent control and its derivatives from the chattering SMC $u(t)$ [43]. It also filters out random noises of small mean values [21, 22].

The variable $w_{n_f+1} = z_0 - f(t)$ is fictitious and is only introduced to keep the same formula for $n_f = 0$. Indeed, in the case $n_f = 0$ DEs (22) disappear and $z_0 - f(t)$ is substituted for w_1 in (23). The resulting derivative estimator is the standard differentiator [33] mentioned above. In particular, $n_d = n_f = 0$ determines the 0-order differentiator $\dot{z}_0 = -\tilde{\lambda}_0 L \,\mathrm{sign}(z_0 - f(t))$, $|\dot{f}_0| \leq L$.

Introduce the short notation for (22), (23)

$$\dot{w} = \Omega_{n_d,n_f}(w, z_0 - f, L), \; \dot{z} = D_{n_d,n_f}(w_1, z, L), \tag{24}$$

for the proper parameters $\tilde{\lambda} = (\tilde{\lambda}_0, ..., \tilde{\lambda}_{n_d+n_f})$ (Fig. 3).

Let $\operatorname{ess\,sup} \eta(t) = \varepsilon_0$ and the maximal allowed sampling-time interval be $\tau > 0$. It is proved in [33, 40] that in that case differentiator (24) in FT provides and holds the accuracy

$$\begin{array}{l} |z_i(t) - f_0^{(i)}(t)| \leq \mu_i L \rho^{n_d+1-i},\ i = 0,1,...,n_d, \\ |w_1(t)| \leq \mu_{w1} L \rho^{n_d+n_f+1} \end{array} \tag{25}$$

for

$$\rho = \max[(\varepsilon_0/L)^{1/(n_d+1)}, \tau], \tag{26}$$

and some constants $\mu_{w1} > 0$, $\mu_i > 0$ only depending on the choice of $\tilde{\lambda}$.

In fact, also internal variables w_k satisfy inequalities $|w_k(t)| \leq \mu_{wk} L \rho^{n_d+n_f+2-k}$, $k = 2,..,n_f$, for some $\mu_{wk} > 0$. Note that these internal variables actually become quite large for general, possibly not bounded, filterable noises [41], but they do not directly influence the outputs z_i. We do not consider such noises in this paper.

Formulas (25) formally stay true for $\tau = 0$ and $\rho = (\varepsilon_0/L)^{1/(n+1)}$ corresponding to continuous-time noisy sampling. Thus, differentiator (27) is exact and asymptotically optimal in spite of its filtering capabilities.

Notation. Recall that for any sampled vector signal $\phi(t_j)$ its increment is denoted by $\delta_j \phi = \phi(t_{j+1}) - \phi(t_j)$.

The discrete differentiator [3]. The discrete version of (24)

$$\begin{array}{l} \delta_j w = \Omega_{n_d,n_f}(w(t_j), z_0(t_j) - f(t_j), L)\tau_j, \\ \delta_j z = D_{n_d,n_f}(w_1(t_j), z(t_j), L)\tau_j + T_{n_d}(z(t_j), \tau_j), \end{array} \tag{27}$$

where the Taylor-like term $T_{n_d} \in \mathbb{R}^{n_d+1}$ is defined as

$$\begin{array}{l} T_{n_d,0} = \frac{1}{2!} z_2(t_j)\tau_j^2 + ... + \frac{1}{n_d!} z_{n_d}(t_j)\tau_j^{n_d}, \\ T_{n_d,1} = \frac{1}{2!} z_3(t_j)\tau_j^2 + ... + \frac{1}{(n_d-1)!} z_{n_d}(t_j)\tau_j^{n_d-1}, \\ \qquad ... \\ T_{n_d,n_d-2} = \frac{1}{2!} z_{n_d}(t_j)\tau_j^2, \\ T_{n_d,n_d-1} = 0,\ T_{n_d,n_d} = 0, \end{array} \tag{28}$$

has the same features as its continuous-time counterpart (24). Terms T_{n_d} are needed in the *stand-alone* numeric-differentiation applications in order to ensure the homogeneity of the discrete error dynamics and the standard continuous-time accuracy (25), (26) with possibly different coefficients μ_i.

4.2 Output feedback stabilization in continuous time

First let σ be only available by its noisy measurements $\hat{\sigma}(t) = \sigma(t, x(t)) + \eta(t)$, $|\eta| \leq \varepsilon_0$. The corresponding FT stabilization is obtained for $\alpha > 0$ large enough and the closed-loop system

$$\begin{aligned}
&\sigma^{(r)} \in [-C, C] + \alpha[K_m, K_M]K_F[u_{*r}](z(t)),\\
&\dot{w} = \Omega_{n_d,n_f}(w, z_0 - \sigma - \eta(t), L),\\
&\dot{z} = D_{r-1,n_f}(w_1, z, L),\\
&L \geq C + K_M\alpha.
\end{aligned} \tag{29}$$

The stabilization is exact for $\eta = 0$. Note that in the case $\eta(t) \equiv 0$ system (29) is homogeneous of the HD -1 and the weights $\deg z_i = \deg \sigma^{(i)} = r - i$, $i = 0, 1, ..., n_d$, $\deg w_k = r + n_f + 1 - k, k = 1, 2, ..., n_f + 1$. Recall that $w_{n_f+1} = z_0 - \hat{\sigma}$ is a fictitious variable. The steady-state system accuracy in the presence of noises is well-known [21, 22, 28] and is described by (20) for $\rho = \varepsilon_0^{1/(n_d+1)}$.

4.3 Output feedback stabilization using discrete differentiators

Let now σ be *discretely sampled* as $\hat{\sigma}(t_j) = \sigma(t_j, x(t_j)) + \eta(t_j)$ for some sampling instants $t_0, t_1, .., \tau_j = t_{j+1} - t_j \leq \tau$, and the bounded noise $|\eta| \leq \varepsilon_0$.

Denote (27), (28) by $\delta_j(w, z)^T = \Delta_{n_d,n_f}(w, z, z_0 - f, L, \tau_j)(t_j)$.

Consider the stabilization of the DI (15) which still evolves in *continuous* time by the feedback zero-hold r-SMC (16) exploiting the discrete differentiator. The closed-loop system contains continuous-time and discrete-time subsystems. Therefore it is a *hybrid* system. It gets the form

$$\begin{aligned}
&\sigma^{(r)} \in [-C, C] + \alpha[K_m, K_M]K_F[u_{*r}](z(t_j)),\ t \in [t_j, t_{j+1}),\\
&\delta_j(w, z)^T = \Delta_{r-1,n_f}(w, z, z_0 - \sigma - \eta, L, \tau_j)(t_j),\\
&L \geq C + K_M\alpha,\ |u_{*r}| \leq 1,\ 0 < \tau_j = t_{j+1} - t_j \leq \tau.
\end{aligned} \tag{30}$$

Now consider the original system (12) of the relative degree r closed by the same feedback. The corresponding closed-loop *hybrid* system gets the form

$$\begin{aligned}
&\dot{x} = a(t, x) + b(t, x)u(t_j), \hat{\sigma}(t_j) = \sigma(t_j, x(t_j)) + \eta(t_j),\\
&u = \alpha u_{*r}(z(t_j)),\ L \geq C + K_M\alpha \sup|u_{*r}|,\ L > 0,\ t \in [t_j, t_{j+1}),\\
&\delta_j(w, z)^T = \Delta_{r-1,n_f}(w(t_j), z_0(t_j) - \hat{\sigma}(t_j), z(t_j), L)\tau_j.
\end{aligned} \tag{31}$$

Theorem 2. *Let the sampling noise satisfy* $|\eta(t)| \leq \varepsilon_0$*, the sampling interval be bounded,* $0 < t_{j+1} - t_j \leq \tau$*,* $n_f \geq 0$*. Then the discrete output feedback control stabilizes both systems* (30) *and* (31) *in FT providing the accuracy* $|\sigma^{(i)}| \leq \gamma_i\rho^{r-i}$*,* $i = 0, 1, ..., r - 1$*, for* $\rho = \max[\varepsilon_0^{1/(n_d+1)}, \tau]$ *and some* $\gamma_0, ..., \gamma_{r-1} > 0$*.*

Addition of the terms $T_{n_f,n_d}(z(t_j), \tau_j)$ is optional and not required in the output feedbacks (31), (30). Unbounded noises are considered in [41].

Note that this theorem is formally extendable also to the limit case $\tau = 0$ corresponding to the continuous sampling of σ in the presence of the Lebesgue-measurable noise $\eta(t)$, $|\eta(t)| \leq \varepsilon_0$. The proof of Theorem 2 is based on the accuracy estimation (66) of the disturbed homogeneous systems (see the Appendix). Also the computer simulation case (complete discretization) is covered there [39, 40].

5 Low-chattering discretization of HOSMs

It is not possible to reasonably define the chattering of a separate signal [36]. Indeed, only the time scaling distinguishes between $\sin(10^6 t)$ and $\sin(10^{-6} t)$. Therefore, we intentionally bound ourselves to the intuitive chattering understanding.

It is well-known that SM control u in average approximates the equivalent control $u_{eq} = -h/g|_{\sigma\equiv 0}$ [60, 43]. Correspondingly in order to exclude the chattering of the ideal Filippov solution for (19), one needs the equivalent u_{eq} itself not to chatter. For the same reason, since measurement noises can mimic the chattering of u_{eq}, one cannot in general remove the control chattering in the presence of noises [36]. We also do not consider the chattering due to parasitic dynamics [7].

Thus our goal is to diminish the high-frequency significant-magnitude vibrations of the SMC (30) *in the case of exact discrete measurements for small enough sampling step τ and relatively slowly changing h, g.*

All available problem solutions are obtained under the same assumptions and prove the system practical stability in the absence of noises. The widespread discontinuity regularization [59] is highly sensitive to noises [36]. Artificial increase of the relative degree [4, 15] raises the sensitivity to noises due to the required higher-order differentiation. Also continuous SM controllers with integral action [45] have differentiation issues and some chattering due to the non-Lipschitzian control.

All Euler-based discretization methods for the discontinuous ODE $\dot{x} = f(t, x)$ require to select a proper value of $\dot{x}(t_j)$ for each sampling/integration time step $x(t_{j+1}) = \dot{x}(t_j)(t_{j+1} - t_j)$. The natural choice $\dot{x}(t_j) = f(t_j, x(t_j))$ inevitably leads to chattering.

The implicit discretization schemes [1, 9] propose a feasible choice of $\dot{x}(t_j)$. The idea is that the knowledge or a proper estimation of the ideal Filippov solution at the next sampling step will allow to choose $\dot{x}(t_j)$ fitting that prediction. The value of $\dot{x}(t_j)$ is chosen in correspondence with the Filippov procedure. It requires numeric solution of nonlinear equations for the proper value of $\dot{x}(t_j)$ at each sampling/integration step. It can be computationally difficult and requires some concrete knowledge of the system. The performance of such algorithms in the presence of noises usually cannot be theoretically established due to the involved numeric procedure.

Our method enlarges the Filippov inclusion, significantly expanding the set of available selections for $\dot{x}(t_j)$ so that no choice affects the standard limit performance of the system as the sampling intervals vanish. Some of these choices significantly reduce the chattering of the approximating solutions. Therefore, one needs to choose such a proper *selector* algorithm for all time instants t_j.

In the following we suggest a simple discretization of the output-feedback SMC (30) *featuring significantly less chattering in the absence of noises and preserving the system performance in the presence of noises.* The case of the direct measurements of $\vec{\sigma}_{r-1}$ is obtained by trivially removing the observer from the feedback.

Also in the sequel *the upper bound τ of the sampling step is assumed available*, whereas the actual sampling steps are variable and unknown.

The proposed alternative discretization should include discretization of both the differentiator [25] and the controller.

5.1 Low-chattering discretization of differentiators

Low chattering discretization of SM-based differentiators is a well-known problem. Until recently it was only solvable by implicit discretization methods [12, 49].

Let $k_L > 0$ be the parameter of the low-chattering differentiator discretization chosen as in [25]. The following is the *low-chattering discrete filtering differentiator* [20]:

$$\begin{array}{l} \delta_j(w,z)^T = \varDelta_{n_d,n_f}(w,z,z_0-f,\hat{L},\tau_j)(t_j), \\ \hat{L}(t_j) = L\,\mathrm{sat}\left(\frac{|w_1(t_j)|}{Lw_\tau}\right),\ w_\tau = k_L\tau^{n_d+n_f+1}. \end{array} \tag{32}$$

Let $|f_0^{n_d+1}| \le L_f \le L$. According to [25] it in FT provides for the accuracy of the form $|z_i - \sigma^{(i)}| \le \mu_{di} L\rho^{r-i}$, $i = 0, ..., r-1$, $\rho = \max[\tau, (\varepsilon_0/L)^{1/(n_d+1)}]$. Here $\varepsilon_0 \ge 0$ is the (unknown) maximal noise amplitude, and $\rho = \tau$ in the absence of noises.

Moreover, if $\varepsilon_0 = 0$, then the new accuracy is $|z_i - \sigma^{(i)}| \le \tilde{\mu}_{di} L_f \tau^{r-i}$, i.e. overestimated values of L do not affect it. Furthermore, if $\lim_{s\to\infty}\sup_{t\ge s}|f_0^{n_d+1}(t)| = 0$ then differentiation errors asymptotically converge to zero, $|z_i - \sigma^{(i)}| \to 0$ [25].

Note that the accuracy estimation holds for any bounded sampling steps and noises, i.e. for any $\rho \ge 0$. In particular, in the limit case of exact continuous-time-measurements $\tau = \varepsilon_0 = 0$ the differentiator becomes exact. Moreover, such differentiator of the differention order 3 and the filtering order 9 is numerically demonstrated to produce 3 asymptotically exact derivatives for the input $\cos(3\ln(t+1))$, the constant sampling step $\tau = 5$ (five), and $L = 1000$ [25].

An optional choice of parameters [25] valid for any $n_d, n_f \ge 0$, $n_d + n_f = 0, 1, ..., 12$, is provided in Figs. 3, 4 which correspond to the sequence of recursive-form [33] parameters $1.1, 1.5, 2, 3, 5, 7, 10, 12, 14, 17, 20, 26, 32, ...$. Recall that increasing k_L preserves the validity of the parameters [25].

n_d+n_f	Parameters $\tilde{\lambda}_0, \tilde{\lambda}_1, ..., \tilde{\lambda}_{n_d+n_f}$ of differentiator												
0	1.1												
1	1.1	1.5											
2	1.1	2.12	2										
3	1.1	3.06	4.16	3									
4	1.1	4.57	9.30	10.03	5								
5	1.1	6.75	20.26	32.24	23.72	7							
6	1.1	9.91	43.65	101.96	110.08	47.69	10						
7	1.1	14.13	88.78	295.74	455.40	281.37	84.14	12					
8	1.1	19.66	171.73	795.63	1703.9	1464.2	608.99	120.79	14				
9	1.1	26.93	322.31	2045.8	6002.3	7066.2	4026.3	1094.1	173.72	17			
10	1.1	36.34	586.78	5025.4	19895	31601	24296	8908	1908.5	251.99	20		
11	1.1	48.86	1061.1	12220	65053	138954	143658	70830	20406	3623.1	386.7	26	
12	1.1	65.22	1890.6	29064	206531	588869	812652	534837	205679	48747	6944.8	623.30	32

Fig. 3 Parameters $\tilde{\lambda}_0, \tilde{\lambda}_1, ..., \tilde{\lambda}_{n_d+n_f}$ of differentiator (22), (23) for $n_d + n_f = 0, 1, ..., 12$

$n_d{+}n_f$	$n_f=0$	$n_f=1$	$n_f=2$	$n_f=3$	$n_f=4,\ldots,n_d{+}n_f$
0	2				
1	1	1			
2	3	3	3		
3	10	6	6	6	
4	50	10	10	10	10
5	3000	400	400	400	400
6	$1.5\cdot10^5$	$2\cdot10^4$	10^4	10^4	10^4
7	$3\cdot10^7$	10^7	10^7	10^7	10^7
8	10^{10}	$1.5\cdot10^{10}$	$1.5\cdot10^9$	$1.5\cdot10^9$	$1.5\cdot10^9$
9	10^{12}	$7\cdot10^{12}$	$5\cdot10^{11}$	$1.5\cdot10^{11}$	$1.5\cdot10^{11}$
10	10^{14}	10^{15}	10^{13}	$3\cdot10^{12}$	$3\cdot10^{12}$
11	$8\cdot10^{15}$	10^{17}	10^{15}	$8\cdot10^{13}$	$2\cdot10^{14}$
12	$3\cdot10^{18}$	$8\cdot10^{18}$	10^{16}	$7\cdot10^{15}$	$7\cdot10^{15}$

Fig. 4 Valid parameters k_L of the discrete differentiator (32) corresponding to Fig. 3

5.2 Low-chattering Discretization of Higher Order SMC.

Consider the closed-loop SMC DI obtained from (31) using controller U_r,

$$\begin{array}{l}\sigma^{(r)} \in [-C,C]+[K_m,K_M]u(t_j), \hat\sigma(t_j)=\sigma(t_j)+\eta(t_j),\\ u=\alpha U_r(z(t_j)),\ L\ge C+K_M\alpha\sup|U_r|,\ L>0,\ t\in[t_j,t_{j+1}),\\ \delta_j(w,z)^T=\mathit{\Delta}_{r-1,n_f}(w(t_j),z_0(t_j)-\hat\sigma(t_j),z(t_j),\hat L(t_j))\tau_j.\end{array} \tag{33}$$

Here $\hat L(t_j)$ is defined by (32). The task is to develop a proper discretization U_r for controllers u_{*r} from (17) and (18).

The main idea is to complement the powers of coordinates $\sigma^{(i)}$ up to one turning controllers u_{*r} defined by (17) or (18) into a linear high-gain control in the infinitisemally small vicinity of the origin depending on $\tau << 1$. Note that similarly to the low-chattering differentiation the results are to hold for any $\tau > 0$.

Each term $\lfloor\sigma^{(i)}\rceil^\gamma, \gamma\in(0,1)$, is replaced with the term $\mathrm{sat}^{1-\gamma}(|\sigma^{(i)}|/\zeta_{\tau i})\lfloor\sigma^{(i)}\rceil^\gamma$. The transformation is performed in infinitesimally thin layers $|\sigma^{(i)}|\le\zeta_{\tau i}$ along the surfaces of discontinuity and/or non-smoothness, which keeps the velocity vectors close to the graph of the Filippov inclusion (19). Since $\lim_{\tau\to0}\zeta_{\tau i}=0$ the distance of the vectors from the graph vanishes as $\tau\to0$, producing a valid discretization (Theorem 1).

Assigning the weights $\deg\tau=\deg t=1$, $\deg\sigma^{(i)}=\deg z_{(i)}=r-i$, $\deg w_j=r+n_f$, and taking $\zeta_{\tau i}=k_i^{r-i}\tau^{r-i}$ for some $k_i>0$, obtain a homogeneously disturbed r-SMC system [39, 40]. It is natural to call such a discretization **homogeneous**. As the result the accuracy of the discretization is established by [40, 39] and coincides with the standard worst-case accuracy of the homogeneous r-SM (20). That worst-case accuracy is improved in the degenerate case when the parameter C from (15) vanishes, which corresponds to the vanishing of the equivalent control. In that particular case, in a small vicinity of the origin $z=\vec\sigma_{r-1}=0$ the system becomes alternatively homogeneous of the zero homogeneity degree and asymptotically stable for correspondingly chosen parameters. That asymptotic stability becomes global, provided parameters are properly assigned.

Discretization of quasi-continuous controllers (17)**.** Outputs z_i of differentiator (32) are substituted for $\sigma^{(i)}$, $i = 0, 1, ..., r-1$,

$$\begin{array}{l}\delta_j(w,z)^T = \Delta_{n_d,n_f}(w,z,z_0-\sigma,\hat{L},\tau_j)(t_j),\\ \hat{L}(t_j) = L\,\mathrm{sat}\left(\frac{|w_1(t_j)|}{Lw_\tau}\right),\ w_\tau = k_L\tau^{n_d+n_f+1},\ L \geq C + K_M\alpha.\end{array} \tag{34}$$

producing the output feedback control. Pick some numbers $\hat{k}_0, ..., \hat{k}_{r-1}, k_h > 0$, $k_h \in (0,1]$, $\kappa_* > 0$, to define the width of the layer $\zeta_{\tau i} = k_i^{r-i}\tau^{r-i}$, $k_i = \kappa_*\hat{k}_i$,

$$\begin{array}{l}u(t) = \alpha\, U_r(z(t_j)),\ t \in [t_j, t_{j+1}),\\ U_r(z) = -\,\mathrm{sat}\left[\frac{Q(z)}{k_hQ_\tau}\right]\frac{P(z)}{Q(z)},\\ Q(z) = |z_{r-1}|^{\frac{1}{1}} + \beta_{r-2}\,\mathrm{sat}(\frac{|z_{r-2}|}{\zeta_{\tau r-2}})^{\frac{1}{2}}|z_{r-2}|^{\frac{1}{2}} + ...\\ \qquad\qquad\qquad\qquad +\beta_0\,\mathrm{sat}(\frac{|z_0|}{\zeta_{\tau 0}})^{\frac{r-1}{r}}|z_0|^{\frac{1}{r}},\\ P(z) = z_{r-1} + \beta_{r-2}\,\mathrm{sat}(\frac{|z_{r-2}|}{\zeta_{\tau r-2}})^{\frac{1}{2}}\lfloor z_{r-2}\rceil^{\frac{1}{2}} + ...\\ \qquad\qquad\qquad\qquad +\beta_0\,\mathrm{sat}(\frac{|z_0|}{\zeta_{\tau 0}})^{\frac{r-1}{r}}\lfloor z_0\rceil^{\frac{1}{r}},\\ \zeta_{\tau i} = k_i^{r-i}\tau^{r-i},\ k_i = \kappa_*\hat{k}_i,\ \hat{k}_i > 0,\ i = 0,1,...,r-1,\ \kappa_* > 0\\ Q_\tau = \zeta_{\tau r-1}^{\frac{1}{1}} + \beta_{r-2}\zeta_{\tau r-2}^{\frac{1}{2}} + ... + \beta_0\zeta_{\tau 0}^{\frac{1}{r}}.\end{array} \tag{35}$$

If $\vec{\sigma}_{r-1}$ are directly measured, system coordinates $\sigma^{(i)}$ are substituted back for z_i in (35), $i = 0.1, ..., r-1$, and (34) is excluded.

After some calculation get

$$Q_\tau = q_\tau\tau,\ q_\tau = k_{r-1} + \beta_{r-2}k_{r-2} + ... + \beta_0k_0.$$

Therefore, in the set $|z_i| \leq (k_i\tau)^{r-i}$, $Q(z) \leq k_hq_\tau\tau$ the control function U_r from (35) gets the form

$$\begin{array}{l}U_r(z) = -(k_hq_\tau\tau)^{-1}[z_{r-1} + \tilde{\beta}_{r-2}\tau^{-1}z_{r-2} + ... + \tilde{\beta}_0\tau^{-(r-1)}z_0],\\ \tilde{\beta}_i = \beta_ik_i^{-(r-1-i)} = \beta_i(\kappa_*\hat{k}_i)^{-(r-1-i)},\ i = 0, 1...., r-2,\end{array} \tag{36}$$

which corresponds to the local output-feedback high-gain control with the small parameters τ, κ_*^{-1}. Note that it only takes place in the discrete form of the control and in a vicinity of $\vec{\sigma}_{r-1} = z = 0$ of the diameter proportional to τ.

Discretization of the relay r-SMC (18)**.** Choose the discretization

$$\begin{array}{l}u(t) = \alpha\, U_r(z(t_j)),\ t \in [t_j, t_{j+1}),\\ U_r(z) = -\,\mathrm{sat}\left[\frac{P(z)}{k_hQ_\tau}\right],\end{array} \tag{37}$$

It is easy to see that in the set $|z_i| < (k_i\tau)^{r-i} = \zeta_{\tau_i}^{r-i}$ the control once more gets the form (36) of the local output-feedback high-gain control with the small parameters τ, κ_*^{-1}. That is also a **homogeneous discretization**.

Clearly any set of $\hat{\beta}_0, ..., \hat{\beta}_{r-2} > 0$ is obtainable by a proper choice of $\hat{k}_0, ..., \hat{k}_{r-1}$. Also, substituting κk_i for k_i, $\kappa > 0$, causes the division of the roots by κ for the polynomial $s^{r-1} + \tilde{\beta}_{r-2} s^{r-2} + ... + \tilde{\beta}_0$.

Theorem 3. *Let $\alpha > 0$, $\beta_0, ..., \beta_{r-2} > 0$ be properly chosen ensuring the FT stability of the DI* (15) *under the QC control* (17) *(respectively the "relay" control* (18)*), the differentiator parameters be also properly chosen [41, 25], in particular, $L > C + K_M \alpha$ holds. Then for any choice of positive numbers $k_0, ..., k_{r-1} > 0$ (i.e. any corresponding k_h, κ_*) and $\tau > 0$ the system* (15), (34), (35) *(respectively* (37)*) establishes the standard accuracy* (20) *for bounded sampling noises, and features the standard filtering capabilities for noises of the filtering orders not larger than $n_f \geq 0$ [41].*

Thus Theorem 3 guaranties the preservation of the standard properties of the homogeneous r-SMC. The following theorem deals with chattering-attenuation capabilities.

Theorem 4. *Let the conditions of Theorem 3 hold, and let $k_i = \kappa_* \hat{k}_i$, $i = 0, ..., r-1$, for some $\kappa_* > 0$, $\hat{k}_0, ..., \hat{k}_{r-1} > 0$, also let $\hat{k}_0, ..., \hat{k}_{r-2} > 0$ generate the Hurwitz polynomial $s^{r-1} + \hat{\beta}_{r-2} s^{r-2} + ... + \hat{\beta}_0$, $\hat{\beta}_i = \beta_i \hat{k}_i^{-(r-1-i)}$. Let also $\hat{k}_{r-1}$ be small enough with respect to $\hat{k}_0, ..., \hat{k}_{r-2}$. Then, provided κ_* and k_h be chosen respectively sufficiently large and sufficiently small and there are no sampling noises the following statements are true for any $\tau > 0$:*

- *The choice $k_i = \kappa_* \hat{k}_i$, $i = 0, 1, ..., r-1$, ensures that the system* (15), (32), (35) *in FT stabilizes in the set $|\sigma^{(i)}| \leq k_i^{r-i} \tau^{r-i}$, $|z_i| \leq k_i^{r-i} \tau^{r-i}$.*
- *System* (15), (32), (35) *which results from discretization, is exponentially stable for $C = 0$ (i.e. $\vec{\sigma}_{r-1}, z \to 0$) for any $k_h \in (0, 1]$ small enough.*

Hence, the steady-state chattering removal is obtained in the absence of noises in the rather rare case, when the equivalent control is identical zero, $u_{eq} = -h(t,x)/g(t,x) \equiv 0$. In general, when $u_{eq} \neq 0$, control u tracks u_{eq}, provided u_{eq} is smooth and slow.

The QC control (17) is smooth outside of the coordinate planes $z_i = 0$ ($\sigma^{(i)} = 0$ for direct measurements) and continuous everywhere except the origin $z = 0$ (respectively $\vec{\sigma}_{r-1} = 0$), correspondingly the proposed discretization is expected to significantly diminish the chattering in the whole state space. In the case of the "relay" control (18) the theorem does not ensure chattering reduction *during the transient* even for $h \equiv 0$. Indeed, no special discretization is applied along the discontinuity set of (18).

5.3 *Proof sketch*

Consider the case of the control (17). The similar case of (18) is simpler.

Consider the auxiliary set-valued homogeneous control function

$$
\begin{array}{l}
u \in \alpha\, \hat{U}_r(z,\epsilon,\epsilon_1),\ \hat{U}_r(z,\epsilon,\epsilon_1) = -[1-\epsilon_1,1]\overline{U}_r(z,\epsilon),\ \ \epsilon_1,\epsilon \in (0,1),\\
\varpi(\vec{z}_{r-2}) = \beta_{r-2}|z_{r-2}|^{\frac{1}{2}} + ... + \beta_0|z_0|^{\frac{1}{r}},\\
\tilde{\varpi}_s(\vec{z}_{r-2},\vec{s}_{r-2}) = \beta_{r-2}\,\mathrm{sat}(\frac{|z_{r-2}|}{s_{r-2}^2})^{\frac{1}{2}}|z_{r-2}|^{\frac{1}{2}} + ... + \beta_0\,\mathrm{sat}(\frac{|z_0|}{s_0^r})^{\frac{r-1}{r}}|z_0|^{\frac{1}{r}},\\
\omega_s(\vec{z}_{r-2},\vec{s}_{r-2}) = \beta_{r-2}\,\mathrm{sat}(\frac{|z_{r-2}|}{s_{r-2}^2})^{\frac{1}{2}}\lfloor z_{r-2}\rceil^{\frac{1}{2}} + ... + \beta_0\,\mathrm{sat}(\frac{|z_0|}{s_0^r})^{\frac{r-1}{r}}\lfloor z_0\rceil^{\frac{1}{r}},\\
\omega(z,\epsilon) = \{\frac{z_{r-1}+\omega_s}{|z_{r-1}|+\tilde{\varpi}_s}\ \Big| s_0,...,s_{r-2} \in [0,\epsilon\varpi(\vec{z}_{r-2})]\},\\
\overline{U}_r(z,\epsilon) = \begin{cases} u_{*r}(z) \text{ for } \epsilon\varpi < |z_{r-1}| < \varpi/\epsilon,\\ [1-\epsilon,1]\,\mathrm{sign}\, z_{r-1} \text{ for } \ \epsilon|z_{r-1}| \geq \varpi,\ z_{r-1} \neq 0,\\ \omega(z,\epsilon) \text{ for } |z_{r-1}| \leq \epsilon\varpi,\ \ \vec{z}_{r-2} \neq 0,\\ [-1,1] \text{ for } z = 0. \end{cases}
\end{array} \tag{38}
$$

It is easy to see that the graph of (38) is close to the graph of $u_{*r}(z)$ over any homogeneous ball for $\epsilon, \epsilon_1 > 0$ small enough. Thus, since (29) is FT stable for $\eta = 0$, also the additionally modified homogeneous system

$$
\begin{array}{l}
\sigma^{(r)} \in [-C,C] + \alpha[K_m,K_M]\,\overline{\mathrm{co}}(\hat{U}_r(z,\epsilon,\epsilon_1) + \mathrm{sign}\, u_{*r}(z)),\\
\dot{w} = \Omega_{n_d,n_f}(w, z_0-\sigma, L),\\
\dot{z} = D_{r-1,n_f}(w_1, z, L)
\end{array} \tag{39}
$$

is FT stable for sufficiently small $\epsilon, \epsilon_1 > 0$. Recall that after a FT transient $\vec{\sigma}_{r-1} \equiv z$ is kept.

Now Theorem 3 directly follows from the properties of homogeneous perturbations of system (39) [40].

Prove Theorem 4. Fix any $\zeta_{\tau i} > 0$, $i = 0,...,r-1$. Consider the perturbation of system (39)

$$
\begin{array}{l}
\sigma^{(r)} \in [-C,C] + \alpha[K_m,K_M]\,\overline{\mathrm{co}}\,\tilde{U}_r(z),\\
\dot{w} = \Omega_{n_d,n_f}(w, z_0-\sigma, L),\\
\dot{z} = D_{r-1,n_f}(w_1, z, L),\\
\tilde{U}_r(z) = \begin{cases} \hat{U}_r(z) + \mathrm{sign}\, u_{*r}(z) \text{ for } \ |z_{r-1}| > \zeta_{\tau\, r-1} \text{ or } |z_{r-1}| \leq \epsilon\varpi(\vec{z}_{r-2}),\\ [-1,1] \ \text{ for } \ |z_{r-1}| \leq \zeta_{\tau\, r-1} \text{ and } |z_{r-1}| > \epsilon\varpi(\vec{z}_{r-2}). \end{cases}
\end{array} \tag{40}
$$

System (40) differs from (39) only in a small vicinity of $z = \vec{\sigma}_{r-1} = 0$. Choosing sufficiently small $\zeta_{\tau\, r-1} > 0$ obtain that the system trajectories stabilize in a small vicinity of the origin inside the set $|z_i| \leq \zeta_{\tau\, i}, z_i = \sigma^{(i)}$, $i = 0, ..., r-2$.

It is easy to see that for sufficiently small $k_h > 0$ we also obtain that $\alpha\, U_r(z) \in \overline{\mathrm{co}}\,\tilde{U}_r(z)$. Thus the continuous analogue of the system (15), (34), (35) also stabilizes in the same set.

Let now $|z_i| \leq \zeta_{\tau\, i}, z_i = \sigma^{(i)}$, $i = 0,...,r-2$ be kept. Opening the saturation functions obtain that in that vicinity of the origin the control gets the form

$$u = -\alpha\,\mathrm{sat}(\frac{Q(z)}{k_h Q_\tau})\frac{z_{r-1}+\hat\beta_{r-2}z_{r-2}+...+\hat\beta_0 z_0}{|z_{r-1}|+\hat\beta_{r-2}|z_{r-2}|+...+\hat\beta_0|z_0|},$$
$$\hat\beta_i = \beta_i(\frac{1}{\zeta_{\tau i}})^{r-1-i},\ i=0,1....,r-2, \tag{41}$$

The corresponding polynomial is Hurwitz, which implies that for $C=0$ the system (15), (41) is always locally AS for sufficiently small k_h [38]. Otherwise, if $C \neq 0$, it converges to a vicinity of zero proportional to C.

Let $C=0$ then the system converges into the vicinity of zero $|z_i| \le \zeta_{\tau\,i}, z_i = \sigma^{(i)}$, $i = 0,...,r-1$. Now all saturation functions can be opened and one gets the equivalent AS linear system. By time transformation one can replace τ with 1 obtaining

$$\dot z_i = z_{i+1},\ i=0,...,r-2,$$
$$\dot z_{r-1} = -(k_h q_\tau)^{-1}[z_{r-1}+\tilde\beta_{r-2}z_{r-2}+...+\tilde\beta_0 z_0], \tag{42}$$
$$\tilde\beta_i = \beta_i k_i^{-(r-1-i)} = \beta_i(\kappa_*\hat k_i)^{-(r-1-i)}.$$

It is AS for sufficiently small $k_h > 0$. Although that by itself does not automatically cause the AS of the Euler discretization for the time steps not exceeding 1, the AS is ensured for κ_* large enough. The same choice also provides the corresponding features of the discretized original homogeneous system [39, 40].

6 Discretization examples for the sliding orders 3, 4

The proposed low-chattering output-feedback SMC discretization is demonstrated here for the kinematic car model ($r=3$) and the integrator chain (academic example, $r=4$) [4].

6.1 Discretization of the 3-SM car control

The example from [23] is studied here for other sampling periods and initial conditions. Consider the kinematic "bicycle" model of the vehicle motion [53]

$$\dot x = V\cos(\varphi),\ \dot y = V\sin(\varphi)$$
$$\dot\varphi = \frac{V}{l}\tan\theta,\quad \dot\theta = u, \tag{43}$$

where x and y are Cartesian coordinates of the rear-axle middle point (Fig. 5), $l = 5\,m$ is the distance between the axles, φ is the orientation angle, $V = 10\ m/s$ is the constant longitudinal velocity, θ is the steering angle (i.e. the actual real-life control), and $u = \dot\theta$ is the auxiliary computer-based control.

The goal is to track some smooth trajectory $y = g(x)$, unknown in advance, whereas $g(x(t)), y(t)$ are sampled in real time. Therefore the task is to make

[4] The model and some parameters are reprinted from the paper [23] by authors with the permission by IEEE.

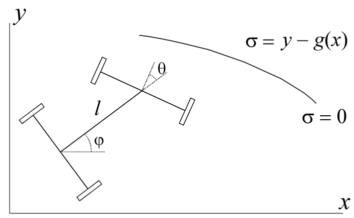

Fig. 5 Kinematic car model and the desired trajectory $y = g(x)$.

$\sigma(x, y) = y - g(x)$ as small as possible. The tracking error σ is measured with the constant sampling step τ. The function $g(x) = 10\sin(0.05x) + 5$ is chosen for the simulation. The output relative degree obviously equals 3.

Control (32), (35) is applied for $r = 3$, $\alpha = 1$, $\beta_1 = 2$, $\beta_0 = 1$, $k_0 = 10^{5/3}$, $k_1 = 4000^{1/2}$, $k_2 = 300$, $k_h = 0.3$, $L = 50$, $n_f = 2$, $k_L = 5$. The control is kept at 0 till $t = 1$ which provides some time for the differentiator convergence, and is applied according to the formula only for $t > 1$.

The initial conditions $(x(0), y(0), \varphi(0), \theta(0)) = (0, -5, -1, -0.4)$, $z(0) = 0, w(0) = 0$ are set. The simulation is performed by the Euler integration method for the integration step 10^{-4}. The discretization time interval τ of the output-feedback control is *different* and is naturally never less than the integration step.

Note that since the differentiator has $n_d + n_f + 1 = 2 + 2 + 1 = 5$ variables, the closed-loop system is of the dimension 4+5=9 and keeps second-order SMs both in the control and the observation contours.

First take $\tau = 0.0001$ and apply control (30) using the standard Euler discretization (5) (Fig. 6a,b,c). The resulting accuracy is described by the component-wise inequality $(|\sigma|, |\dot{\sigma}|, |\ddot{\sigma}|) \leq (3.4 \cdot 10^{-8}m, 1.4 \cdot 10^{-4}m/s, 0.024\, m/s^2)$. Now apply the proposed new discretization. The performance is shown on the left of Fig. 6 in Fig. 6d,e,f. The corresponding accuracies are $(|\sigma|, |\dot{\sigma}|, |\ddot{\sigma}|) \leq (1.4 \cdot 10^{-8}m, 1.3 \cdot 10^{-4}m/s, 1.0 \cdot 10^{-5}m/s^2)$. One observes that the trajectories are exactly the same, whereas the chattering is practically removed.

The performance of the both standard and new discretizations for the sampling step $\tau = 0.03$ is shown in Fig. 7. Recall that the integration step of the whole system is still 10^{-4} mimicking the continuous-time dynamics of the controlled process. The resulting accuracy for the standard discretization is $(|\sigma|, |\dot{\sigma}|, |\ddot{\sigma}|) \leq (0.45m, 1.2m/s, 6.3m/s^2)$. The new discretization yields the accuracy $(|\sigma|, |\dot{\sigma}|, |\ddot{\sigma}|) \leq (0.37m, 0.23m/s, 0.16m/s^2)$. Also here no visible chattering is present in spite of the large discretization step. The proposed discretization actually preserves the system performance from 6d,e,f.

6.2 *Integrator Chain Control,* $r = 4$

Consider the standard integrator chain

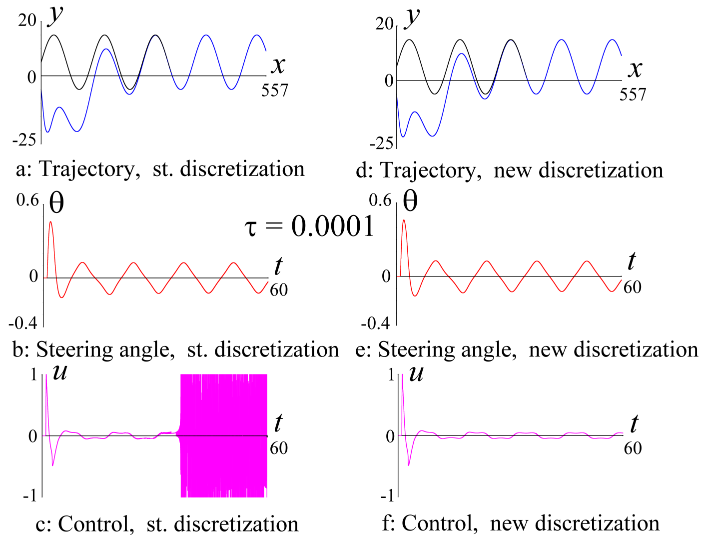

Fig. 6 a: 3-SM car control, car trajectory and control for the coinciding sampling step $\tau = 10^{-4}$ and the integration step. a,b,c: standard Euler discretization, d,e,f: new discretization.

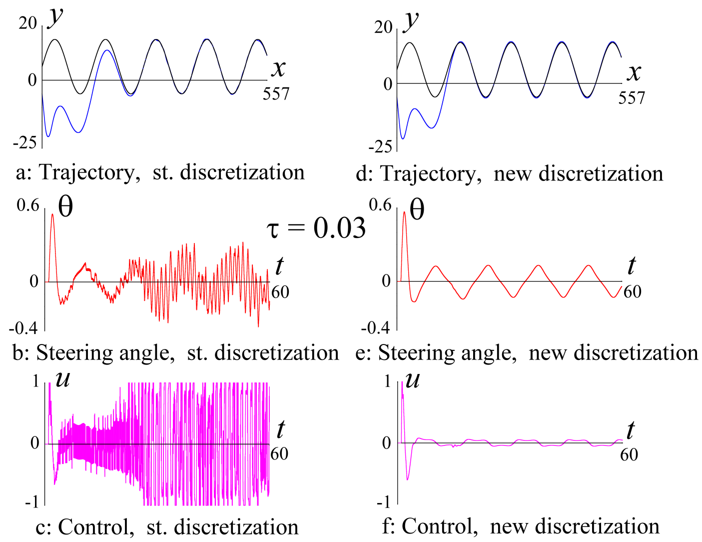

Fig. 7 a: 3-SM car control, car trajectory and control (steering angle derivative), sampling step $\tau = 0.03$, integration step 10^{-4}. a,b,c: standard Euler discretization, d,e,f: new discretization. New discretization keeps the performance from Fig. 6 in spite of the much larger sampling step.

$$\sigma^{(4)} = h(t, \vec{\sigma}_3) + (1.5 - \cos(\sigma\dot{\sigma}))u, |h| \le 1. \tag{44}$$

Let the whole state $\vec{\sigma}_3$ be available. The initial value $\vec{\sigma}_3(0) = (4, -7, 9, -3)$ is taken. The integration/sampling step is $\tau = 10^{-4}$ in all simulations.

Choose the 4-SM "relay" control

$$u = -10\,\mathrm{sign}(\dddot{\sigma} + 2\lfloor\ddot{\sigma}\rceil^{\frac{1}{2}} + 2\lfloor\dot{\sigma}\rceil^{\frac{1}{3}} + \lfloor\sigma\rceil^{\frac{1}{4}}). \tag{45}$$

Let $k_0 = 10^2$, $k_1 = (\frac{2}{3})^{\frac{1}{2}} \cdot 10^2$, $k_2 = \frac{2}{3} \cdot 10^2$, $k_3 = 1$, and $k_h = 0.3$, $\zeta_{\tau i} = k_i^{4-i}\tau^{4-i}$, $\;i = 0, 1, 2, 3$. According to (37) the proposed new discretization of the control is

$$u = -10\ \mathrm{sat}\left(\frac{\dddot{\sigma} + 2\,\mathrm{sat}(\frac{|\ddot{\sigma}|}{\zeta_{\tau 2}})^{\frac{1}{2}}\lfloor\ddot{\sigma}\rceil^{\frac{1}{2}} + 2\,\mathrm{sat}(\frac{|\dot{\sigma}|}{\zeta_{\tau 1}})^{\frac{2}{3}}\lfloor\dot{\sigma}\rceil^{\frac{1}{3}} + \mathrm{sat}(\frac{|\sigma|}{\zeta_{\tau 0}})^{\frac{3}{4}}\lfloor\sigma\rceil^{\frac{1}{4}}}{k_h\left(\zeta_{\tau 3} + 2\zeta_{\tau 2}^{\frac{1}{2}} + 2\zeta_{\tau 1}^{\frac{1}{3}} + \zeta_{\tau 0}^{\frac{1}{4}}\right)}\right) \tag{46}$$

First consider the case when $h \neq 0$, Fig. 8,

$$h = 0.5\cos(t + \dot{\sigma}). \tag{47}$$

Starting from $t = 20$ the standard discretization produces the accuracy

$$(|\sigma|, |\dot{\sigma}|, |\ddot{\sigma}|, |\dddot{\sigma}|) \le (1.5 \cdot 10^{-11}, 8 \cdot 10^{-9}, 8 \cdot 10^{-6}, 8 \cdot 10^{-3}). \tag{48}$$

whereas the new discretization leads to the accuracy

$$(|\sigma|, |\dot{\sigma}|, |\ddot{\sigma}|, |\dddot{\sigma}|) \le (1.5 \cdot 10^{-9}, 1.5 \cdot 10^{-9}, 1.5 \cdot 10^{-9}, 1.5 \cdot 10^{-9}). \tag{49}$$

The case $h = 0$, Fig. 9. In that case, the standard dicretization starting from $t = 20$ implies the same accuracy (48), whereas the new discretization implies asymptotic convergence and the accuracy

$$(|\sigma|, |\dot{\sigma}|, |\ddot{\sigma}|, |\dddot{\sigma}|) \le (3 \cdot 10^{-20}, 10^{-19}, 3 \cdot 10^{-19}, 7 \cdot 10^{-18}) \text{ for } t \ge 20. \tag{50}$$

Note that as we note in Section 5.2, discretization (46) is not intended to remove the chattering during the transient.

7 Discretization of the Twisting Controller

Let $r = 2$. Then (15) gets the form

$$\ddot{\sigma} \in [-C, C] + \alpha[K_m, K_M]K_F[u_{*2}](\sigma, \dot{\sigma}), \tag{51}$$

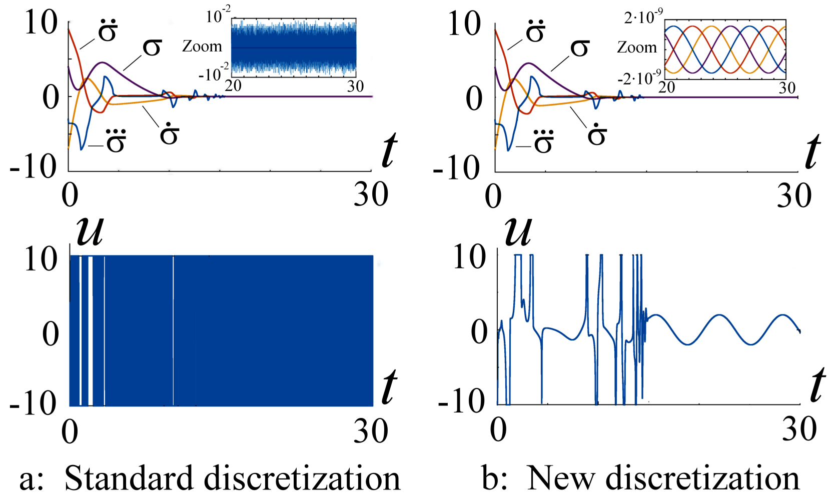

Fig. 8 4-SM stabilization of the system (44) for $h = 0.5 \cdot \cos(t + \dot{\sigma})$.

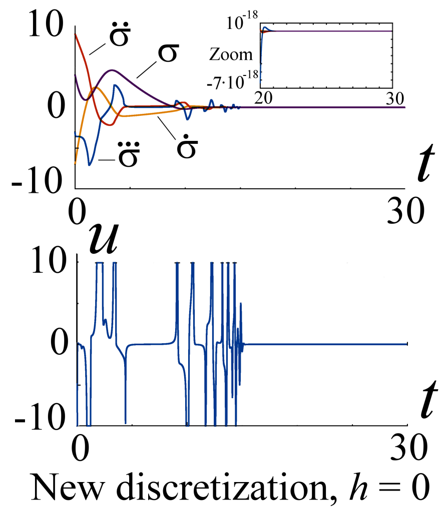

Fig. 9 Asymptotic stabilization of the system (44) for $h \equiv 0$ by the new discretization.

where the control can be, in particular, chosen in the form (17) or (18). The second one coincides with the homogeneous version of the popular terminal SMC [44].

Another option is to apply the twisting controller [32]

$$\begin{aligned} &u_{*2} = U_{Tw} = -\beta_0 \operatorname{sign}\sigma - \beta_1 \operatorname{sign}\dot{\sigma}, \beta_0 > \beta_1 > 0; \\ &\alpha(\beta_0 - \beta_1)K_m > C,\ \tfrac{\alpha(\beta_0+\beta_1)K_m - C}{\alpha(\beta_0-\beta_1)K_M + C} > 1. \end{aligned} \tag{52}$$

Here the second line contains practically necessary and sufficient conditions for its FT convergence [32, 33] (only the equality cases are excluded).

Choose any $k_0, k_1 > 0$. Then the obvious discretization is

$$U_{twd}(t) = -\beta_0 \operatorname{sat}\left(\tfrac{\sigma(t_j)}{k_0^2\tau^2}\right) - \beta_1 \operatorname{sat}\left(\tfrac{\dot{\sigma}(t_j)}{k_1\tau}\right),\ t \in [t_j, t_{j+1}). \tag{53}$$

It is also a **homogeneous discretization**, since defining $\deg\tau = \deg t$ renders (53) homogeneous. Correspondingly in a small vicinity of $\sigma = \dot{\sigma} = 0$ the control becomes a linear Hurwitz controller. In the case $C = 0$ an AS system of the zero homogeneity degree is produced. The corresponding theorems and the proofs are very similar to Section 5, but are much simpler.

7.1 Case study: targeting

In the following example discretization (53) is modified in order to account for the targeting-dynamics specifics: both h and g from (13) escape to infinity as the target is approached.

Consider the geometry of the relative motion of missile (M) and target (T) in the vertical interception plane x, y (Fig. 10). Both objects are formally described as point masses.

The planar missile-target engagement kinematics is described by the relative displacement vector $\vec{r}_R$ and its derivatives $\vec{v}_R, \vec{a}_R$

$$\begin{aligned} &\vec{r}_R = \vec{r}_T - \vec{r}_M, \quad \vec{v}_R = \vec{v}_T - \vec{v}_M, \quad \vec{a}_R = \vec{a}_T - \vec{a}_M, \\ &\dot{\vec{v}}_M = \vec{a}_M,\ \dot{\vec{v}}_T = \vec{a}_T,\ \dot{\vec{v}}_R = \vec{a}_R, \\ &\dot{\vec{r}}_M = \vec{v}_M,\ \dot{\vec{r}}_T = \vec{v}_T,\ \dot{\vec{r}}_R = \vec{v}_R. \end{aligned} \tag{54}$$

Here indexes M, T and R mean "missile", "target" and "relative", $\vec{r}_T$, $\vec{v}_T$, $\vec{a}_T$, $\vec{r}_M$, $\vec{v}_M$, $\vec{a}_M$, $\vec{r}_R$, $\vec{v}_R$, $\vec{a}_R \in \mathbb{R}^2$.

Consider the polar coordinates (r, λ), where r is the range from the missile to the target along the line of sight (LOS), and λ is the LOS angle with respect to the horizontal plane (the axis x). During the attack the impact angle is quite small, and the dynamic equation for $\lambda(t)$ is obtained from the plane kinematics of rigid bodies [46],

$$\ddot{\lambda} = -\frac{2}{r}\dot{\lambda}\dot{r} + \frac{1}{r}(a_{T\lambda} - a_{M\lambda}). \tag{55}$$

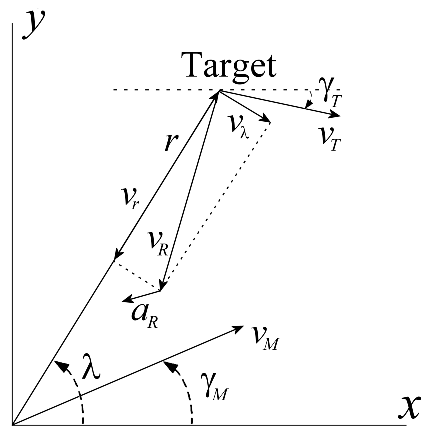

Fig. 10 Planar engagement geometry

Here $a_{T\lambda}$, $a_{M\lambda}$ are the target and the missile acceleration components orthogonal to the LOS.

It is well known that the direct hit is assured, provided $\dot\lambda = 0$ is kept. Correspondingly, *the goal is to make* $\dot\lambda$ *vanish and keep it at zero.*

Assume real-time direct measurements of λ and r (from a seeker). Let the control u be the derivative of the missile acceleration component a_m orthogonal to the missile velocity $\vec{v}_M$. Let γ_M be the angle between $\vec{v}_M$ and the axis x. The corresponding dynamics are

$$\begin{array}{l} \ddot\lambda = -\frac{2}{r}\dot\lambda\dot r + \frac{1}{r}(a_{T_\lambda} - a_m\cos(\lambda-\gamma_M)), \\ \dot a_m = u. \end{array} \tag{56}$$

Correspondingly the guidance task is reduced to steering the system (56) to the manifold $\dot\lambda = 0$. I.e. let $\sigma = \dot\lambda$. Obviously the system relative degree is 2.

Apply a second-order filtering differentiator (22), (23) of some filtering order n_f with the input λ and the outputs z_0, z_1, z_2 estimating $\lambda, \dot\lambda, \ddot\lambda$ respectively. The corresponding structure of the output-feedback twisting controller is

$$u = \alpha(\beta_0 \operatorname{sign} z_1 + \beta_1 \operatorname{sign} z_2). \tag{57}$$

The differentiator parameter L is chosen so as to provide for the inequality $|\dddot\lambda| \le L$ during the targeting mission. In the close proximity of the target the differentiator inevitably diverges.

While the standard discretization of the control is obvious, the proposed alternative controller discretization is

$$\tilde u = \alpha(\beta_0 \operatorname{sat}\frac{z_1\cdot r}{K_1\tau^2\alpha} + \beta_1 \operatorname{sat}\frac{z_2\cdot r}{K_2\tau\alpha}), \tag{58}$$

where $\tau > 0$ is once more the upper bound of the sampling step and $K_1, K_2 > 0$ are some proper gains.

7.2 Simulation of Targeting Control

Let the initial position of the missile be at the origin $x = 0[m], y = 0[m]$, and the initial position of the target be at the point $x = 4000[m], y = 2500[m]$. The initial velocities of the missile and the target are $200[m/s]$ and $150[m/s]$, respectively. The initial velocity angles of the missile and the target are $45[deg]$ and $180[deg]$, respectively. The maximal normal acceleration of the missile is $20[m/sec^2]$, both the missile and the target are subjects to the gravitation. The Euler integration step is 10^{-6} in all simulations.

Let a_t be the component of the missile acceleration along the missile velocity. Correspondingly one gets

$$\begin{aligned}
&\dot{a}_m = u,\\
&\dot{\vec{v}}_M = [a_m \cos(\gamma_M + \tfrac{\pi}{2}), a_m \sin(\gamma_M + \tfrac{\pi}{2}) + g]^T,\\
&\dot{\vec{r}}_M = \vec{v}_M(t),\\
&\dot{\vec{v}}_T = \vec{a}_T = [a_t \cos(\gamma_T(t) + \tfrac{\pi}{2}), a_t \sin(\gamma_T(t) + \tfrac{\pi}{2}) + g]^T,\\
&\dot{\vec{r}}_T = \vec{v}_T(t).
\end{aligned} \tag{59}$$

Here r, λ, γ satisfy the relations

$$r = \|r_R\|,\ \lambda = \tan^{-1}(\tfrac{r_{R_y}}{r_{R_x}}),\ \gamma_M = \tan^{-1}(\tfrac{v_{M_y}}{v_{M_x}}),\ \gamma_T = \tan^{-1}(\tfrac{v_{T_y}}{v_{T_x}}). \tag{60}$$

Intercepting maneuvering target. Let the target maneuver with the acceleration

$$a_t(t) = 75\cos(2\pi f t) \tag{61}$$

of the amplitude $75[m/s^2]$ and the frequency $0.5[Hz]$. The maximal lateral acceleration of the missile is $100[m/s^2]$.

Let the controller parameters be $\beta_0 = 5$, $\beta_1 = 2$, $\alpha = 50$. Apply the filtering differentiator (24) of the differentiation order $n_d = 2$, the filtering order $n_f = 2$ with the Lipschitz parameter $L = 100$.

First assume that r, λ are sampled with the sampling time step $\tau = 10^{-6}$ which equals the integration step. The standard discretization of the controller produces the missing distance of $2{\cdot}10^{-5}[m]$. The interception trajectories, the missile acceleration, and the missile acceleration derivative (the control) are shown in Fig. 11 on the left.

Taking the sampling step $\tau = 10^{-3}$ get a miss distance of $1.35 \cdot 10^{-4}[m]$. The interception geometry, the missile acceleration and the control (missile acceleration command derivative) are shown in the middle of Fig. 11.

The performance of the proposed new discretization (58) for $K_1 = 2000$, $K_2 = 100$ is shown on the right of Fig. 11. The corresponding miss distance is $1.63 \cdot 10^{-4}[m]$.

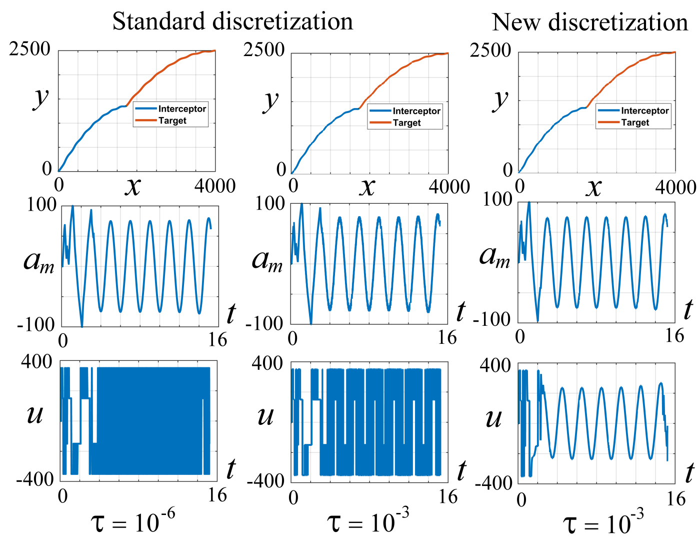

Fig. 11 Intercepting maneuvering target. Standard discretization: $\tau = 10^{-6}$, $\tau = 10^{-3}$. New discretization: $\tau = 10^{-3}$.

Intercepting ballistic target. Change the setup assuming that the target does not maneuver, i.e. $a_t(t) \equiv 0$. Take $\alpha = 20$ and the larger sampling step $\tau = 10^{-2}$. The standard discretization results in the miss distance of $0.0675[m]$. The corresponding targeting performance is shown on the left of Fig. 12. The proposed new discretization results in the miss distance of $1.63 \cdot 10^{-4}[m]$ (Fig. 12 on the right). The new discretization leads to much smoother missile acceleration a_m and $u = \dot{a}_m$.

8 Conclusions

The proposed low-chattering discretization of Filippov discontinuous systems is computationally simple, guaranties the preservation of system trajectories, stability and accuracy.

Contrary to other known discretization approaches the standard HOSM uncertainty conditions are enough, the sampling steps are not required to be equal or to be known in advance.

Only an upper bound for the sampling intervals is required to be known, but there are no restrictions on its value, and it can be very rough. The control or system

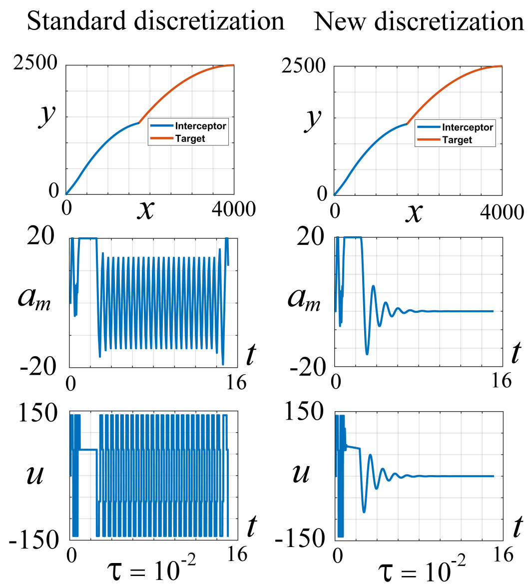

Fig. 12 Intercepting ballistic target. The standard discretization (on the left) and the new discretization (on the right) are performed with the sampling step $\tau = 10^{-2}$.

discretization are performed by the formulas known in advance. No solution of any equation is required at each sampling step.

Sampling noises do not destroy the system performance, and the theoretical system accuracy estimations are preserved. At the same time the attenuation of chattering in the presence of significant noise in general is impossible.

The main result of the paper is Theorem 1 which establishes the new discretization approach. Its proof is almost trivial, but it opens infinitely many practical options for the low-chattering practical SMC discretization in real-life industrial applications.

The approach has been applied for the low-chattering dicretization of general single-input single-output nonlinear systems of any relative degree. Two families of homogeneous SM controllers were considered and the corresponding discretizations were proposed. Theorem 3 assures that no choice of parameters can destroy the standard system performance, whereas possibly leaving the chattering intact, Theorem 4 establishes the chattering attenuation for suitable controlled processes.

Simulation of the 3-SM car control and 4-SMC stabilization of an integrator chain are demonstrated. The new control discretization successfully suppresses the chattering of the 3-SM car control and keeps the trajectories visually the same for the sampling periods 0.0001 and 0.03. The SMC chattering is significantly reduced, at the same time improving the system accuracy in the absence of noises, and preserving the standard system accuracy in their presence.

Another example is the low-chattering discretization of the twisting controller. The discretization is applied for targetting maneuvering and ballistic missiles.

Appendix: Introduction to the weighted homogeneity

Following is the brief presentation of the homogeneity theory [5]. Assign the *weights (degrees)* $m_1, m_2, \ldots, m_{n_x} > 0$ to the coordinates $x_1, x_2, \ldots, x_{n_x}$ of $\mathbb{R}^{n_x}$, and denote $\deg x_i = m_i$. *Dilations* [2] are defined as the simplest linear transformations

$$d_\kappa(x) = (\kappa^{m_1} x_1, \kappa^{m_2} x_2, ..., \kappa^{m_{n_x}} x_{n_x}), \tag{62}$$

depending on the parameter $\kappa \geq 0$.

It is said that the function $f : \mathbb{R}^{n_x} \to \mathbb{R}^m$ is of the *homogeneity degree* (HD) (*weight*) $q \in \mathbb{R}$, $\deg f = q$, if the equality $f(x) = \kappa^{-q} f(d_\kappa x)$ holds identically for any $x \in \mathbb{R}^{n_x}$, $\kappa > 0$.

The notions of a vector function $f : \mathbb{R}^{n_x} \to \mathbb{R}^{n_x}, f : x \mapsto f(x) \in \mathbb{R}^{n_x}$, and a vector field $f : \mathbb{R}^{n_x} \to T\mathbb{R}^{n_x}, f : x \mapsto f(x) \in T_x\mathbb{R}^{n_x}$ are distinguished [56].

A vector-set function $F(x) \subset \mathbb{R}^m$ is termed *homogeneous* of the HD $q \in \mathbb{R}$, if the equality $F(x) = \kappa^{-q} F(d_\kappa x)$ holds identically for any $x \in \mathbb{R}^{n_x}$, $\kappa > 0$ [34].

On the other hand, a vector-set field $F(x) \subset T_x\mathbb{R}^{n_x}$ (DI (1), $\dot{x} \in F(x)$) is termed *homogeneous* of the HD $q \in \mathbb{R}$, if the equality $F(x) = \kappa^{-q} d_\kappa^{-1} F(d_\kappa x)$ holds identically for any x and $\kappa > 0$ [34].

That definition implies that $\frac{d}{d(\kappa^{-q} t)} d_\kappa x \in F(d_\kappa x)$ holds, i.e. DI (1) does not change under the homogeneous time-coordinate transformation $(t, x) \mapsto (\kappa^{-q} t, d_\kappa x), \ \ \kappa > 0$. Correspondingly we often interpret $-q$ as the weight of the time t, $\deg t = -q$, and the weight $\deg t$ can be positive, negative or zero.

The weight $\deg 0$ is not defined (can be any number), whereas for any constant $a \neq 0$ get $\deg a = 0$.

One easily checks the simple rules of the homogeneous arithmetic: $\deg A^a = a \deg A$, $\deg(AB) = \deg A + \deg B$, $\deg \frac{\partial}{\partial \alpha} A = \deg A - \deg \alpha$, $\deg \dot{A} = \deg A - \deg t$.

A vector field $f(x) \in T_x\mathbb{R}^{n_x}$ is treated as a particular case of a vector-set field $F(x) \subset T_x\mathbb{R}^{n_x}$ when the set $F(x)$ has only one element, $F(x) = \{f(x)\}$. Thus, in the case of the vector field $f(x)$ and the differential equation (DE) $\dot{x} = f(x) = (f_1(x), f_2(x), ..., f_{n_x}(x))^T$ the classical weighted homogeneity $\deg \dot{x}_i = \deg x_i - \deg t$, $i = 1, 2, ..., n_x$ is obtained.

Homogeneous norm is defined as any continuous positive-definite function of the HD 1. It is not a norm in the standard sense. In this paper homogeneous norms are denoted as $||x||_h$. Each two homogeneous norms $||\cdot||_h$ and $||\cdot||_{h*}$ are equivalent in the proportionality sense: there exist such $\gamma_*, \gamma^* > 0$ that inequalities $\gamma_* ||x||_{h*} \leq ||x||_h \leq \gamma^* ||x||_{h*}$ hold any $x \in \mathbb{R}^{n_x}$.

Two standard homogeneous norms are

$$||x||_{h\infty} = \max_{1 \leq i \leq n_x} \{|x_i|^{\frac{1}{m_i}}\}, \ ||x||_{h\varpi} = (\sum_i |x|^{\frac{\varpi}{m_i}})^{\frac{1}{\varpi}}.$$

[5] Standard notions introduced here are partially reprinted from the papers [21, 23] by authors with the permission by Springer Nature and IEEE.

Note that $||x||_{h\varpi}$ is continuously differentiable for $x \neq 0$, if $\varpi > \max\{m_i\}$.

The weights and HDs are defined up to proportionality. Let $\deg x_i = m_i, -\deg t = q$, then for any $\gamma > 0$ the redefinition $\deg x_i = \gamma m_i, -\deg t = \gamma q$ implies that HDs of all functions/fields/inclusions are simply multiplied by γ. Correspondingly homogeneous norms are not preserved.

r-SM homogeneity. Under assumptions (14) system (12) of the relative degree r satisfies (13). Choose any control (16). The corresponding closed-loop DI (15)

$$\begin{aligned} &\sigma^{(r)} \in [-C, C] + [K_m, K_M]u, \\ &u = -\alpha u_{*r}(\vec{\sigma}_{r-1}). \end{aligned} \tag{63}$$

can be made homogeneous by a proper weights asignment.

The presence of the segment $[-C, C]$, $C > 0$, on the right-hand side of (63) implies that $\deg \sigma^{(r)} = 0$. On the other hand $\deg \sigma^{(r)} = \deg \sigma - r \deg t$. It implies that $\deg t > 0$. Let $\deg t = 1$ and the system HD be -1. Then the only possible weights are $\deg \sigma = r$, $\deg \dot{\sigma} = r - 1$, ..., $\deg \sigma^{(r-1)} = 1$.

Furthermore, $\deg u_{*r} = 0$ is necessarily to hold, which implies that

$$\begin{aligned} &\forall \kappa > 0 \; \forall \vec{\sigma}_{r-1} \in \mathbb{R}^r : \quad u_{*r}(\vec{\sigma}_{r-1}) \equiv u_{*r}(\hat{d}_\kappa \vec{\sigma}_{r-1}), \\ &\hat{d}_\kappa \vec{\sigma}_{r-1} = (\kappa^r \sigma, \kappa^{r-1}\dot{\sigma}, ..., \kappa \sigma^{(r-1)}). \end{aligned} \tag{64}$$

A function $f : \mathbb{R}^{n_x} \to \mathbb{R}^{m_x}$ is *quasi-continuous* (QC) [35], if it is continuous everywhere except the origin $x = 0$. In particular, all continuous functions are QC.

A homogeneous DI (1) is AS (FTS, FxTS), if the origin $x = 0$ is its global AS (FTS, FxTS) equilibrium.

A set D_0 is termed *homogeneously retractable* if $d_\kappa D_0 \subset D_0$ for any $\kappa \in [0, 1]$.

A Filippov DI (1) is called *contractive* [34], if for some numbers $T, \varepsilon > 0$, there exist such a retractable compact D_0 and a compact D_1, $0 \in D_1$, $D_1 + B_\varepsilon \subset D_0$ that for any solution $x(t)$ the starting-point placement $x(0) \in D_0$ implies that $x(T) \in D_1$.

A Filippov DI $\dot{x} \in \tilde{F}(x)$ is termed a *small homogeneous perturbation* of the homogeneous Filippov DI $\dot{x} \in F(x)$, if the set $\tilde{F}(x)$ is close to $F(x)$ in some vicinity of $x = 0$. It formally means that whenever $x \in B_1$ the relation $\tilde{F}(x) \subset F(x) + B_\varepsilon$ holds for some small $\varepsilon \geq 0$.

The following theorem [39, 40, 19] describes the relations between the contractivity, stability and the HD sign.

Theorem 5. *Consider the homogeneous Filippov DI* (1) *of the HD q. Then its asymptotic stability (AS) and contractivity features are equivalent and robust to small homogeneous perturbations. Moreover,*

- *AS implies FT stability if $q < 0$, and FT stability implies that $q < 0$;*
- *if $q = 0$ AS is exponential;*
- *if $q > 0$ AS implies the FxT attractivity of any ball B_ε, $\varepsilon > 0$, but the convergence to the origin is slower than exponential.*

Any AS homogeneous Filippov DI possesses a differentiable homogeneous Lyapunov function [2, 5].

Accuracy of perturbed homogeneus DIs. Consider the retarded "noisy" perturbation of the AS Filippov homogeneous DI (1) of the negative HD $q < 0$ [34]

$$\dot{x} \in F(x(t - [0, \tau]) + B_{h\varepsilon}),\ x \in \mathbb{R}^{n_x}, \tag{65}$$

where $\tau, \varepsilon \geq 0$, $B_{h\varepsilon} = \{x \in \mathbb{R}^{n_x} \mid ||x||_h \leq \varepsilon\}$.

In principle DI (65) requires some functional initial conditions for $t \in [-\tau, 0]$. Correspondingly the following result [33] imposes some homogeneity assumptions on these conditions [17, 40] which are always satisfied provided the solutions do not depend on the solution prehistory for $t < 0$. That assumption usually holds in the case of sampled systems comprised of smooth dynamic systems closed by digital dynamic controllers, which in their turn exploit discrete output sampling starting at $t = 0$.

So assume that the solutions of (65) are independ of the values $x(t)$ for $t < 0$, and fix any homogeneous norm $|| \cdot ||_h$. Then the accuracy

$$x \in \gamma B_{h\rho},\ \rho = \max[\varepsilon, \tau^{-1/q}], \tag{66}$$

is established in FT for some $\gamma > 0$ independent of ε, τ and initial conditions.

That accuracy is established for $\rho = \varepsilon$ and any sufficiently small τ [17]. If $q > 0$ one still takes $\rho = \varepsilon$, but the initial value $x(0)$ and ε are to be uniformly bounded, whereas τ is to be sufficiently small for each fixed R, $x(0) \in B_R$ (it is the most problematic case [17], since the system can escape to infinity faster than any exponent [37]). A similar result is also true for the implicit Euler discretization with the sampling step τ [17].

References

1. Acary, V., Brogliato, B.: Implicit Euler numerical scheme and chattering-free implementation of sliding mode systems. Systems & Control Letters **59**(5), 284–293 (2010)
2. Bacciotti, A., Rosier, L.: Liapunov Functions and Stability in Control Theory. Springer Verlag, London (2005)
3. Barbot, J.P., Levant, A., Livne, M., Lunz, D.: Discrete differentiators based on sliding modes. Automatica **112**, 108,633 (2020). DOI https://doi.org/10.1016/j.automatica.2019.108633
4. Bartolini, G., Ferrara, A., Usai, E.: Chattering avoidance by second-order sliding mode control. IEEE Transactions on Automatic Control **43**(2), 241–246 (1998)
5. Bernuau, E., Efimov, D., Perruquetti, W., Polyakov, A.: On homogeneity and its application in sliding mode control. Journal of the Franklin Institute **351**(4), 1866–1901 (2014)
6. Boiko, I.: Frequency domain analysis of fast and slow motions in sliding modes. Asian Journal of Control **5**(4), 445–453 (2003)
7. Boiko, I., Fridman, L.: Analysis of chattering in continuous sliding-mode controllers. IEEE Transactions on Automatic Control **50**(9), 1442–1446 (2005)
8. Boiko, I., Fridman, L., Pisano, A., Usai, E.: Analysis of chattering in systems with second-order sliding modes. IEEE transactions on Automatic control **52**(11), 2085–2102 (2007)

9. Brogliato, B., Polyakov, A.: Digital implementation of sliding-mode control via the implicit method: A tutorial. International Journal of Robust and Nonlinear Control **31**(9), 3528–3586 (2021)
10. Brogliato, B., Polyakov, A., Efimov, D.: The implicit discretization of the super-twisting sliding-mode control algorithm. IEEE Transactions on Automatic Control **65**(8), 3707–3713 (2019)
11. Byun, G., Kikuuwe, R.: An improved sliding mode differentiator combined with sliding mode filter for estimating first and second-order derivatives of noisy signals. International Journal of Control, Automation and Systems **18**(12), 3001–3014 (2020)
12. Carvajal-Rubio, J., Sánchez-Torres, J., Defoort, M., Djemai, M., Loukianov, A.: Implicit and explicit discrete-time realizations of homogeneous differentiators. International Journal of Robust and Nonlinear Control **31**(9), 3606–3630 (2021)
13. Clarke, F., Ledayev, Y., Stern, R.: Asymptotic stability and smooth Lyapunov functions. Journal of Differential Equations **149**(1), 69–114 (1998)
14. Ding, S., Levant, A., Li, S.: Simple homogeneous sliding-mode controller. Automatica **67**(5), 22–32 (2016)
15. Dorel, L., Levant, A.: On chattering-free sliding-mode control. In: 47th IEEE Conference on Decision and Control, 2008, pp. 2196–2201 (2008)
16. Drakunov, S., Utkin, V.: On discrete-time sliding modes. In: Nonlinear Control Systems Design 1989, pp. 273–278. Elsevier (1990)
17. Efimov, D., Levant, A., Polyakov, A., Perruquetti, W.: Discretization of asymptotically stable homogeneous systems by explicit and implicit Euler methods. In: 55th IEEE Conference on Decision and Control, CDC'2016, Las-Vegas, December 12-14 (2016)
18. Filippov, A.: Differential Equations with Discontinuous Right-Hand Sides. Kluwer Academic Publishers, Dordrecht (1988)
19. Hanan, A., Jbara, A., Levant, A.: New homogeneous controllers and differentiators. In: Variable-Structure Systems and Sliding-Mode Control, pp. 3–28. Springer, Cham (2020)
20. Hanan, A., Jbara, A., Levant, A.: Non-chattering discrete differentiators based on sliding modes. In: Proc. of the 59th IEEE Conference on Decision and Control, Jeyu Island, December 14-18, Korea, 2020, pp. 3987–3992 (2020)
21. Hanan, A., Jbara, A., Levant, A.: Homogeneous sliding modes in noisy environments. In: Emerging Trends in Sliding Mode Control Theory and Application, pp. 1–46. Springer, Cham (2021)
22. Hanan, A., Jbara, A., Levant, A.: Homogeneous sliding modes in noisy environments, preprint (2021). `https://www.tau.ac.il/~levant/Hanan,Jbara,Levant-Homogeneous_SMC_in_noise,Springer,2021.pdf`
23. Hanan, A., Jbara, A., Levant, A.: Low-chattering discretization of sliding mode control. In: Proc. of the 60th IEEE Conference on Decision and Control (CDC), Austin, TX, USA, December 15-17, 2021, pp. 6403–6408 (2021)
24. Hanan, A., Jbara, A., Levant, A.: Homogeneous low-chattering sliding mode discretization. In: Proc. of the 61th IEEE Conference on Decision and Control (CDC), Cancun, Mexico, December 6-9, 2022, pp. 4276–4281 (2022)
25. Hanan, A., Levant, A., Jbara, A.: Low-chattering discretization of homogeneous differentiators. IEEE Transactions on Automatic Control **67**(6), 2946–2956 (2021)
26. Huber, O., Acary, V., Brogliato, B.: Lyapunov stability and performance analysis of the implicit discrete sliding mode control. IEEE Transactions on Automatic Control **61**(10), 3016–3030 (2015)
27. Isidori, A.: Nonlinear control systems I. Springer Verlag, New York (1995)
28. Jbara, A., Levant, A., Hanan, A.: Filtering homogeneous observers in control of integrator chains. International Journal of Robust and Nonlinear Control **31**(9), 3658–3685 (2021)
29. Kikuuwe, R., Pasaribu, R., Byun, G.: A first-order differentiator with first-order sliding mode filtering. IFAC-PapersOnLine **52**(16), 771–776 (2019)
30. Kikuuwe, R., Yamamoto, Y., Brogliato, B.: Implicit implementation of nonsmooth controllers to nonsmooth actuators. IEEE Transactions on Automatic Control **67**(9), 4645–4657 (2022)
31. Kikuuwe, R., Yasukouchi, S., Fujimoto, H., Yamamoto, M.: Proxy-based sliding mode control: a safer extension of PID position control. IEEE Transactions on Robotics **26**(4), 670–683 (2010)

32. Levant, A.: Sliding order and sliding accuracy in sliding mode control. International J. Control **58**(6), 1247–1263 (1993)
33. Levant, A.: Higher order sliding modes, differentiation and output-feedback control. International Journal of Control **76**(9/10), 924–941 (2003)
34. Levant, A.: Homogeneity approach to high-order sliding mode design. Automatica **41**(5), 823–830 (2005)
35. Levant, A.: Quasi-continuous high-order sliding-mode controllers. IEEE Trans. Aut. Control **50**(11), 1812–1816 (2005)
36. Levant, A.: Chattering analysis. IEEE Transactions on Automatic Control **55**(6), 1380–1389 (2010)
37. Levant, A.: On fixed and finite time stability in sliding mode control. In: Proc. of the 52 IEEE Conference on Decision and Control, Florence, Italy, December 10-13, 2013 (2013)
38. Levant, A.: Non-Lyapunov homogeneous SISO control design. In: 56th Annual IEEE Conference on Decision and Control (CDC), Melbourne, VIC, Australia, Dec. 12-15 , 2017, pp. 6652–6657 (2017)
39. Levant, A., Efimov, D., Polyakov, A., Perruquetti, W.: Stability and robustness of homogeneous differential inclusions. In: Proc. of the 55th IEEE Conference on Decision and Control, Las-Vegas, December 12-14, 2016 (2016)
40. Levant, A., Livne, M.: Weighted homogeneity and robustness of sliding mode control. Automatica **72**(10), 186–193 (2016)
41. Levant, A., Livne, M.: Robust exact filtering differentiators. European Journal of Control **55**(9), 33–44 (2020)
42. Levant, A., Livne, M., Yu, X.: Sliding-mode-based differentiation and its application. IFAC-PapersOnLine **50**(1), 1699–1704 (2017)
43. Levant, A., Yu, X.: Sliding-mode-based differentiation and filtering. IEEE Transactions on Automatic Control **63**(9), 3061–3067 (2018)
44. Man, Z., Paplinski, A., Wu, H.: A robust MIMO terminal sliding mode control scheme for rigid robotic manipulators. IEEE Transactions on Automatic Control **39**(12), 2464–2469 (1994)
45. Mercado-Uribe, J., Moreno, J.: Discontinuous integral action for arbitrary relative degree in sliding-mode control. Automatica **118**, 109,018 (2020)
46. Meriam, J., Kraige, L.: Engineering Mechanics - Dynamics, 7th Edition. Wiley (2012)
47. Miranda-Villatoro, F., Brogliato, B., Castanos, F.: Multivalued robust tracking control of lagrange systems: Continuous and discrete-time algorithms. IEEE Transactions on Automatic Control **62**(9), 4436–4450 (2017)
48. Miranda-Villatoro, F., Brogliato, B., Castanos, F.: Set-valued sliding-mode control of uncertain linear systems: continuous and discrete-time analysis. SIAM Journal on Control and Optimization **56**(3), 1756–1793 (2018)
49. Mojallizadeh, M., Brogliato, B., Acary, V.: Time-discretizations of differentiators: Design of implicit algorithms and comparative analysis. International Journal of Robust and Nonlinear Control **31**(16), 7679–7723 (2021)
50. Polyakov, A., Efimov, D., Brogliato, B.: Consistent discretization of finite-time and fixed-time stable systems. SIAM Journal on Control and Optimization **57**(1), 78–103 (2019)
51. Polyakov, A., Efimov, D., Perruquetti, W.: Finite-time and fixed-time stabilization: Implicit Lyapunov function approach. Automatica **51**(1), 332–340 (2015)
52. Polyakov, A., Fridman, L.: Stability notions and Lyapunov functions for sliding mode control systems. Journal of The Franklin Institute **351**(4), 1831–1865 (2014)
53. Rajamani, R.: Vehicle Dynamics and Control. Springer Verlag, New York (2005)
54. Ríos, H., Teel, A.: A hybrid observer for fixed-time state estimation of linear systems. In: 2016 IEEE 55th Conference on Decision and Control (CDC), pp. 5408–5413. IEEE (2016)
55. Ríos, H., Teel, A.: A hybrid fixed-time observer for state estimation of linear systems. Automatica **87**, 103–112 (2018)
56. Shtessel, Y., Edwards, C., Fridman, L., Levant, A.: Sliding mode control and observation. Birkhauser, Basel (2014)
57. Shtessel, Y., Shkolnikov, I.: Aeronautical and space vehicle control in dynamic sliding manifolds. International Journal of Control **76**(9/10), 1000–1017 (2003)

58. Sira-Ramírez, H.: On the dynamical sliding mode control of nonlinear systems. International Journal of Control **57**(5), 1039–1061 (1993)
59. Slotine, J.J., Li, W.: Applied Nonlinear Control. Prentice Hall Int, New Jersey (1991)
60. Utkin, V.: Sliding Modes in Control and Optimization. Springer Verlag, Berlin, Germany (1992)
61. Xiong, X., Kikuuwe, R., Kamal, S., Jin, S.: Implicit-Euler implementation of super-twisting observer and twisting controller for second-order systems. IEEE Transactions on Circuits and Systems II: Express Briefs **67**(11), 2607–2611 (2019)